Available online at www.sciencedirect.com
SCIENCE DIRECT®
Biochemical and Biophysical Research Communications 324 (2004) 1340–1345
BBRC
www.elsevier.com/locate/ybbrc

Characterization of novel squamous cell carcinoma antigen-related molecules in mice

Y. Sakata[a], K. Arima[a], K. Takeshita[a], T. Takai[b], S. Aoki[c], H. Ogawa[b], H. Sugihara[c], K. Fujimoto[d], K. Izuhara[a,e,*]

[a] *Division of Medical Biochemistry, Department of Biomolecular Sciences, Saga Medical School, Saga 849-8501, Japan*
[b] *Atopy (Allergy) Research Center, Juntendo University, Tokyo 113-8421, Japan*
[c] *Division of Cellular and Molecular Pathology, Department of Pathology and Biodefence, Saga Medical School, Saga 849-8501, Japan*
[d] *Division of Gastroenterology, Department of Internal Medicine, Saga Medical School, Saga 849-8501, Japan*
[e] *Division of Medical Research, Center for Comprehensive Community Medicine, Saga Medical School, Saga 849-8501, Japan*

Received 20 September 2004

Abstract

The squamous cell carcinoma antigen 1 (SCCA1) and SCCA2 are unique serpins that can inhibit cysteine proteinases. SQN-5, their mouse ortholog, has already been identified, and its inhibitory property has been characterized; however, its biological role has remained undefined. Furthermore, no other mouse homolog of SQN-5 has been known. We characterize three mouse members of SCCA-related molecules including SQN-5 in this article. Serpinb3a (SQN-5) and Serpinb3b, but not Serpinb3c, were functional, inhibiting both serine and cysteine proteinases with different inhibitory profiles due to the difference of two amino acids in their reactive site loops. Serpinb3a was ubiquitously expressed in most tissues, whereas expression of Serpinb3b was limited to keratinocytes. Keratinocytes secreted both SCCA-related proteins, Serpinb3a and Serpinb3b. These results indicate that Serpinb3a and Serpinb3b may play different roles by inhibiting intrinsic or extrinsic proteinases with different expression distributions and different inhibitory profiles.

Keywords: Serpin; Proteinase; SCCA1; SCCA2; SQN-5; Serpinb3a; Serpinb3b; Keratinocyte; Reactive site loop

The squamous cell carcinoma antigen 1 (SCCA1: SERPINB3) and SCCA2 (SERPINB4) belong to the ovalbumin-serpin (serine proteinase inhibitors) family, and these proteins are 91% identical at the amino acid level [1]. Both genes locate very closely at human chromosome 18q21.3, suggesting that either gene could arise from the other by gene duplication [2]. Target proteinases for most serpins are the chymotrypsin family of serine proteinases, so a serpin inhibiting cysteine proteinase is defined as a cross-class serpin. Both SCCA1 and SCCA2 inhibit cysteine proteinases such as cathepsin K, L, and S, or Der p 1 and Der f 1, respectively [3–5]. Therefore, SCCA1 and SCCA2 are defined as cross-class serpins, indicating their unique properties.

The biological roles of SCCA1 and SCCA2 remain obscure. It is thought that SCCA1 and SCCA2 play a role in limiting injury by inhibiting lysosomal cysteine proteinases such as cathepsin K, L, and S, or a cationic neutral serine proteinase synthesized by neutrophils and mast cells, cathepsin G [1,4]. We recently found that expression of SCCA1 and SCCA2 was upregulated by two Th2-type cytokines, IL-4 and IL-13, in human bronchial epithelial cells (HBECs) and keratinocytes [6] (K. Mitsuishi et al., unpublished data).

* Corresponding author. Fax: +81 952 34 2058.
E-mail address: kizuhara@med.saga-u.ac.jp (K. Izuhara).

0006-291X/$ - see front matter © 2004 Elsevier Inc. All rights reserved.
doi:10.1016/j.bbrc.2004.09.204

We furthermore demonstrated that SCCA2 inhibited the cysteine proteinase activities of Der p 1 and Der f 1, group I allergens derived from house dust mites, *Dermatophagoides pteronyssinus* and *Dermatophagoides farinae*, respectively [5]. Taking these results together, we assume that SCCA1 and SCCA2 may protect against extrinsic proteinases derived from microbes or parasites involved in the defense mechanism of IL-4 and IL-13.

In contrast to SCCA1 and SCCA2, only one mouse SCCA-related molecule, SQN-5, now denoted as Serpinb3a, has been identified [7,8]. Serpinb3a was 60% and 61% identical with SCCA1 and SCCA2, respectively, and it inhibited both cysteine proteinases such as cathepsin S, K, L, and V, and serine proteinases such as human mast cell chymase (HMC) and cathepsin G. These findings suggested that Serpinb3a had mixed properties of SCCA1 and SCCA2, and that Serpinb3a was also a cross-class serpin. It was reported that Serpinb3a was broadly expressed in most organs at the mRNA level [7]. However, the biological roles of Serpinb3a remained undefined. Furthermore, no other mouse homolog of Serpinb3a was known.

To address these questions, we tried to identify novel mouse homologs of Serpinb3a in silico. It turned out that there existed two novel homologous cDNAs, and we analyzed the inhibitory properties as serpins of their deduced proteins, the expression profiles of these genes, and their induction by IL-4 and IL-13. During the preparation of this manuscript, Askew et al. [9] presented identification of novel genes homologous to Serpinb3a. In this article, we named our three molecules following their nomenclature.

Materials and methods

Materials. Papain, cathepsin G, cathepsin L, and HMC were purchased from Sigma (St. Louis, MO), Calbiochem (San Diego, CA), Athens Research and Technology (Athens, GA), and Cortex Biochem (San Leandro, CA), respectively.

Generation of the proteins of the Serpinb3 members and the Der p 1 protein. Serpinb3a cDNA was prepared by PCR using cDNA derived from mouse lung according to a previous report [8]. *Serpinb3b* and *Serpinb3c* cDNAs were prepared from two RIKEN FANTOM clones, AK003220 and AK003650, from K.K. Danaform (Ibaraki, Japan). These three cDNAs were incorporated into pGEX(-KG)-4T (Amersham Biosciences, Piscataway, NJ). Mutants of Serpinb3a and Serpin b3b were generated by oligonucleotide-directed mutagenesis using two complemented primers with mutations, as previously described [5,10]. Purification of glutathione *S* transferase (GST)-fused proteins of wild and mutated types of the Serpinb3 members was performed as described before [10].

Recombinant Der p 1 protein was generated as described before [11]. Der p 1-N52Q, in which Asn52 was replaced with Gln, diminishing the N-glycosylation site, was used in all experiments.

Enzyme assays. Enzyme assays were performed as described previously [5,10]. The substrates used for enzyme assays of papain, cathepsin L, and Der p 1 were benzoyl-Arg-7-amino-4-methylcoumarin (Bz-R-MCA), benzyloxycarbonyl-Phe-Arg-methylcoumarin (Z-FR-MCA), and butyloxycarbonyl-Gln-Arg-methylcoumarin (Boc-QAR-MCA), respectively. Succinyl-Ala-Ala-Pro-Phe-methylcoumarin (Suc-AAPF-MCA) was used for cathepsin G and HMC. All were purchased from Peptide Institute.

Generation of anti-Serpinb3a serum. Purified GST-fused Serpinb3a protein was used together with complete Freund's adjuvant (Sigma) for immunization of New Zealand White rabbits. Anti-Serpinb3a serum was cross-reacted with Serpinb3b and Serpinb3c.

Reverse transcription-PCR. Total RNA was extracted from each mouse organ by ISOGEN (Nippongene, Tokyo, Japan), followed by the phenol:chloroform extraction. The reverse transcription (RT) reaction primed with random hexamer was performed using a GeneAmp RNA PCR Kit (Applied Biosystems Japan, Tokyo, Japan). The PCR was performed with cDNA as a template using the indicated primers after an initial 5 min denaturation at 95 °C, followed by the indicated cycles of 95 °C for 1 min, the indicated annealing temperature for 1 min, and 72 °C for 1 min. The cycles used were 40, 40, and 23, for Serpinb3a, Serpinb3b, and GAPDH, respectively. The annealing temperatures used were 60, 56, and 55 °C for Serpinb3a, Serpinb3b, and GAPDH, respectively. The PCR primers used were 5′-CATTTGTTTGCTGAAGCCACTAC-3′ and 5′-CATGTTCGAAATCCAGTGATTCC-3′ for Serpinb3a, 5′-ATTCGTTTTCATGCAGCTGATGT-3′ and 5′-GAAAGCTGAAGTTAAATTTGTTTCG-3′ for Serpinb3b, and 5′-GCACCACCAACTGCTTAGCC-3′, and 5′-GATGCAGGGATGATGTTCTGG-3′ for GAPDH, respectively.

Culture of mouse primary keratinocytes. Mouse keratinocytes were obtained and cultured by modifying the previous method [12]. Back skin removed from 2-day newborn C57/BL6 mice or tail skin removed from adult C57/BL6 mice was washed with Modified Eagle's Medium (MEM, Invitrogen, Carlsbad, CA) and cut down. Then the skin was incubated with MEM containing 2 U/ml dispase (Invitrogen), 100 U/ml penicillin G (BANYU Pharmaceutical, Tokyo, Japan), 100 μg/ml streptomycin (Meiji Seika, Tokyo, Japan), and 250 ng/ml amphotericin B (Invitrogen) at 4 °C for 10 h. After the skin was washed by MEM, epidermis and dermis were peeled from it. Keratinocytes were obtained from the epidermis incubated with 0.25% trypsin and 0.02% EDTA in PBS at 37 °C for several minutes, followed by filtration. Fibroblasts were obtained from the dermis cultured with F-12 nutrient mixture (Ham's F-12, Invitrogen) containing 10% FCS, 100 U/ml penicillin G, and 100 μg/ml streptomycin. Keratinocytes were cultured by a double-dish culture system. In this system, mouse fibroblasts were cultured as a feeder layer on the bottom of the outer dish, and keratinocytes were cultured with F-12 Nutrient Mixture containing 10% FCS, 100 U/ml penicillin G, and 100 μg/ml streptomycin, on type I collagen gel (Nitta Gelatin, Osaka, Japan), on the bottom of the inner dish.

Immunostaining. Mouse keratinocytes were fixed on slides by 4% paraformaldehyde (Wako, Osaka, Japan). The sections were pretreated with 0.3% Triton X-100 (Wako) at 4 °C for 5 min. The sections were probed with 50-fold diluted anti-Serpinb3a serum, followed by incubation with FITC-labeled gout anti-rabbit IgG (Southern Biotechnology Associates, Birmingham, AL). The section was mounted with VECTASHIELD H-100 (Vector Laboratories, Burlingame, CA) and the localization of SCCA-related protein was analyzed by Carl Zeiss Axiophoto (Carl Zeiss, Oberkochen, Germany).

Transfection. HEK293T cells were maintained in Dulbecco's modified Eagle's medium supplemented with 10% FCS, 100 μg/ml streptomycin, and 100 U/ml penicillin. Transient expression of Serpinb3a or Serpinb3b into HEK293T was performed by TransFast transfection reagent (Promega, Madison, WI).

Immunoprecipitation and Western blotting. Procedures of immunoprecipitation and Western blotting were carried out as previously described [13]. The proteins were immunoprecipitated from the culture medium of mouse primary keratinocytes from C57/BL6 mice by anti-Serpinb3a serum. The immunoprecipitates were applied to SDS-PAGE and then electrophoretically transferred to polyvinylidene difluoride membranes (Amersham Biosciences, Piscataway, NJ). The membranes were blotted by 100-fold diluted anti-Serpinb3a serum.

The proteins were visualized by enhanced chemiluminescence (ECL, Amersham Biosciences).

Results and discussion

Localization and organization of the genes of Serpinb3 members

We first surveyed the SQN-5 homolog by BLAST search, and found that two novel cDNAs homologous with SQN-5 were inserted into two RIKEN FANTOM clones, AK003220 and AK003650. The homologies of the deduced amino acids of AK003220 and AK003650 with SQN-5 were 87% and 82%, respectively. Askew et al. have very recently demonstrated that there exist four Serpinb3 members including SQN-5, two novel homologs that we had found, and another homolog that we had not recognized, named Serpinb3a, b, c, and d, respectively [9]. The localization and organization of these four genes were verified by a survey using BLAST search. The genes of *Serpinb3a, d, b,* and *c* were localized sequentially in this turn at 60 cM on chromosome 1 (Fig. 1A). The locations of *Serpinb3c* and *Serpinb3a* genes were adjacent to *Serpinb7* and *Serpinb5* genes, respectively, and together with *Serpinb8* and *Serpinb2* genes, these genes made a cluster of Serpin clade b genes. All *Serpinb3b*, *Serpinb3c*, and *Serpinb3c* genes were composed of 8 exons, as was the *Serpinb3a* gene [7] (Fig. 1B). These results indicated that the four genes encoding Serpinb3 members would have arisen by gene multiplication, as the two genes encoding SERPINB3 and SERPINB4 are assumed to be evoked by gene duplication.

Functional analyses of Serpinb3 members

To perform functional analyses of Serpinb3 members, we expressed and purified recombinant proteins of GST-fused Serpinb3a, b, and c. The purity of these three proteins was greater than 95%, as estimated by Coomassie brilliant blue staining (data not shown). We examined the inhibitory effects of these three proteins on two cysteine proteinases, cathepsin L and Der p 1, and two serine proteinases, cathepsin G and HMC. Serpinb3a inhibited all proteinase activities, whereas Serpinb3b inhibited proteinase activities of cathepsin L and cathepsin G, but not Der p 1 and HMC (Fig. 2). Serpinb3c did not inhibit any activity of these four proteinases. None of the three Serpinb3 members inhibited papain. These results suggested that both Serpinb3a and Serpinb3b were able to inhibit both serine and cysteine proteinases, and that Serpinb3a and Serpinb3b showed different inhibitory profiles. It meant that both Serpinb3a and Serpinb3b belonged to cross-class serpins as well as SCCA1 and SCCA2. Askew et al. [9] have reported that neither Serpinb3c nor Serpinb3d performed any inhibitory activity. Together with our present finding, there is no evidence thus far that Serpinb3c is a functional serpin.

Preference of amino acids in the reactive site loop sequences of Serpinb3a and Serpinb3b

The inhibitory mechanism of the serpin is well characterized [14]. The exposed reactive site loop (RSL) of the serpin is recognized by the proteinase, and a 'bait' peptide bond (P1–P1′) that mimics the normal substrate of the proteinase is attacked by the active serine residue of the proteinase. By either forming an acyl-enzyme intermediate linked by an oxy-ester bond or cleaved by the proteinase just as the substrate of the proteinase, the serpin inhibits the target proteinases. It is well known that different inhibitory profiles of SCCA1 and SCCA2 are due to the different amino acid sequences of their RSLs [5,10,15]. Although only two amino acids were different among the 13 amino acids of the RSL sequences of Serpinb3a and Serpinb3b (Table 1), it

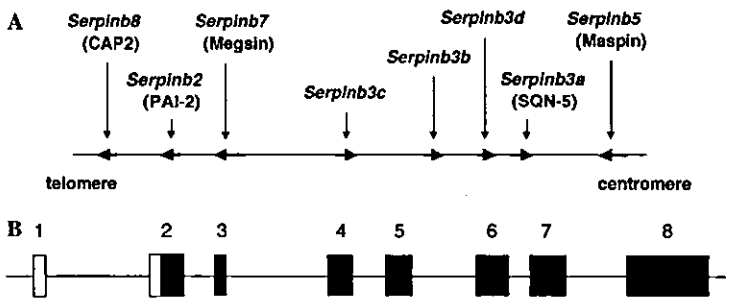

Fig. 1. Mapping and organization of the genes of the Serpinb3 family. (A) Mapping of the genes of the Serpinb3 family and the adjacent genes on chromosome 1 is depicted. CAP2 and PAI-2 represent cytoplasmic antiproteinase 2 and plasminogen activator inhibitor-2, respectively. (B) Organization of the exon/intron of the Serpinb3 family genes is shown. The exon numbers are depicted, and the closed boxes represent the portion of the open reading frame.

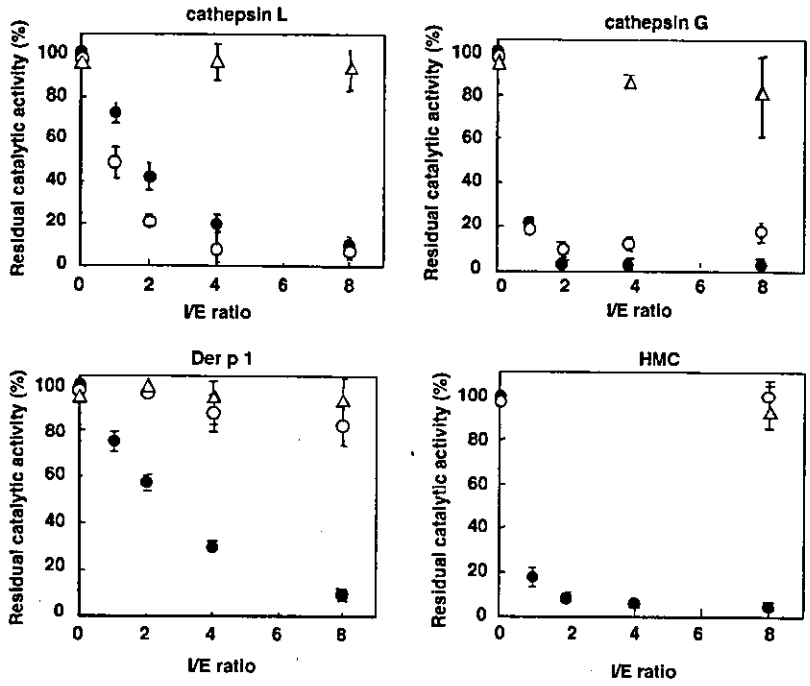

Fig. 2. Inhibitory activity of Serpinb3a, Serpinb3b, and Serpinb3c. Cathepsin L (5 nM), cathepsin G (40 nM), Der p 1 (10 nM), and HMC (40 nM) were incubated with either Serpinb3a (closed circles) or Serpinb3b (open circles) or Serpinb3c (open triangles) at the indicated I/E ratio. The residual enzyme activities are depicted.

Table 1
Alignment of RSLs of the mutants and their inhibitory activities

Position	Proximal hinge							Reactive site loop													Distal hinge	CatL	CatG	Derpl	HMC
	14	13	12	11	10	9	8	7	6	5	4	3	2	1	1′	2′	3′	4′	5′	6′					
Human																									
SCCA1	G	A	E	A	A	A	A	T	A	V	V	G	F	G	S	S	P	T	S	T	H	+++	–	–	–
SCCA2	.	V	.	.	.	.	.	.	.	.	.	V	V	E	L	.	S	P	.	.	C	–	+++	++	+++
Mouse																									
Serpinb3a	G	T	E	A	A	A	A	T	G	V	E	V	S	L	T	S	A	Q	I	A	C	+++	+++	++	+++
Serpinb3aL351V	.	.	.	.	.	.	.	.	.	.	.	.	.	V	T	.	.	.	.	.	.	ND	ND	++	+++
Serpinb3aT352R	.	.	.	.	.	.	.	.	.	.	.	.	.	L	R	.	.	.	.	.	.	ND	ND	+	+
Serpinb3b	.	.	.	.	.	.	.	.	.	.	.	.	.	V	R	.	.	.	.	.	.	+++	+++	–	–
Serpinb3bV351L	.	.	.	.	.	.	.	.	.	.	.	.	.	L	R	.	.	.	.	.	.	ND	ND	–	–
Serpinb3bR352T	.	.	.	.	.	.	.	.	.	.	.	.	.	V	T	.	.	.	.	.	.	ND	ND	+	+
Serpinb3c	.	.	.	.	D	P	.	S	.	E	.	.	I	L	R	L	.	.	V	.	R	–	–	–	–

Bold letter, mutated amino acid; ND, not determined.

was assumed that the different properties of Serpinb3a and Serpinb3b on HMC and Der p 1 were due to the difference of these two amino acids in their RSL sequences. To explore this possibility, we exchanged either Leu351 or Thr352 corresponding to Serpin b3a with Val or Arg corresponding to Serpinb3b, or vice versa, and analyzed their inhibitory effects on HMC and Der p 1 (Table 1). When Thr352 in Serpinb3a was replaced with Arg, the mutated type drastically decreased its inhibitory activity, whereas replacement of Leu351 with Val did not affect it. In contrast, when Arg352 in Serpinb3b was replaced with Thr, the mutated type partially recovered the inhibitory effect, whereas no recovery was observed when exchanging Val351 with Leu. These results demonstrated that Thr352 in the RSL of Serpinb3a was critical for its inhibitory activity on HMC and Der p 1.

Expression of Serpinb3a and Serpinb3b

It is known that SCCA1 and SCCA2 were co-expressed broadly in normal tissues: the epithelium of tongue, tonsil, esophagus, uterine cervix, vagina, and the

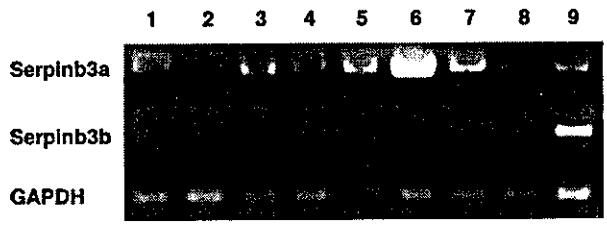

Fig. 3. Expression of Serpinb3a and Serpinb3b. Total RNA was extracted from each organ, and then RT-PCR for Serpinb3a, Serpinb3b, and GAPDH was performed. The numbers represent (1) liver, (2) kidney, (3) spleen, (4) heart, (5) lung, (6) thymus, (7) intestine, (8) muscle, and (9) keratinocytes.

conducting airways; Hassall's corpuscles of the thymus; and some areas of the skin [16]. It has been reported that Serpinb3a is also expressed broadly at the mRNA level [7]. We next analyzed the expression of Serpinb3a and Serpinb3b in each organ at the mRNA level. The homology between Serpinb3a and Serpinb3b was as high as 93%, so we developed a RT-PCR method that could distinguish expression of Serpinb3a and Serpinb3b (data not shown). When we analyzed liver, kidney, spleen, heart, lung, thymus, intestine, muscle, and keratinocytes, expression of Serpinb3a was observed in all investigated organs or cells, most strongly in thymus (Fig. 3). In contrast, among the examined samples Serpinb3b was expressed only in keratinocytes. These results demonstrated that although Serpinb3a and Serpinb3b were highly homologous, the transcriptional regulations of Serpnb3a and Serpinb3b were different.

Secretion of SCCA-related proteins in keratinocytes

We recently found that expression of SCCA1 and SCCA2 was upregulated in skin lesion of atopic dermatitis patients and that epidermal keratinocytes were the main source of SCCA production in skin lesions (K. Mitsuishi, unpublished data). The present finding that both Serpinb3a and Serpinb3b were co-expressed in keratinocytes at the mRNA level prompted us to investigate their protein production in mouse keratinocytes. When keratinocytes derived from infant and adult mice were cultured in vitro, keratinocytes showed positive staining for anti-Serpinb3a serum, but not pre-immune serum (Fig. 4A). We previously indicated the possibility that HBECs secreted the SCCA proteins [6]. To address whether mouse keratinocytes also secrete SCCA-related proteins, we analyzed the existence of SCCA-related proteins in the cultured medium of mouse keratinocytes (Fig. 4B). The mobility of Serpinb3a was slightly faster than that of Serpinb3b. A doublet-band corresponding to the sizes of Serpinb3a and Serpinb3b was detected in the cultured medium of mouse keratinocytes. These results suggested that mouse keratinocytes generated and secreted Serpinb3a and Serpinb3b proteins at almost equal levels.

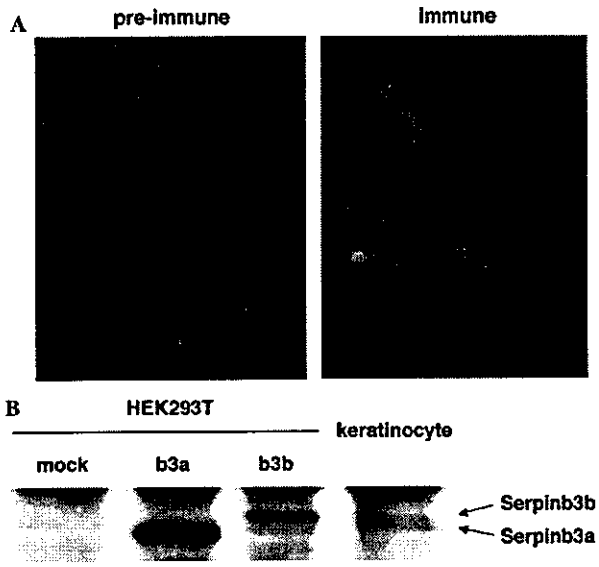

Fig. 4. Production and secretion of Serpinb3a and Serpinb3b from mouse keratinocytes. (A) Immunostaining of SCCA-related molecules in mouse keratinocytes by anti-Serpinb3a serum or pre-immune serum is shown. The fluorescence images are depicted. (B) Culture media were prepared from Serpinb3a- or Serpinb3b-transfected HEK293T cells or mouse keratinocytes, and then immunoprecipitates of anti-Serpinb3a serum were subjected to Western blotting using anti-Serpinb3a serum.

Recently, we showed that IL-4 and IL-13 had an ability to induce expression of SCCA1 and SCCA2 in human keratinocytes and HBECs [6] (K. Mitsuishi, unpublished data). Thus, we explored the possibility that expression of Serpinb3a or Serpinb3b was also augmented by IL-4 and IL-13 in mouse keratinocytes; however, IL-4 and IL-13 did not affect their expression (data not shown). These results demonstrated that expression mechanism of SCCA-related genes was different in mice and humans; *SERPINB3* and *SERPINB4* genes were induced by IL-4 and IL-13 in humans, whereas *Serpinb3* genes were constitutively expressed in mice. It may indicate that biological roles of IL-4 and IL-13 are different in mice and humans in the expression of proteinase inhibitors.

Acknowledgments

We thank Dr. Dovie R. Wylie for a critical review of the manuscript. We also thank Drs. Takehiro Fujise, Toshihiro Kondo, Ko Okumura, and Takeshi Kato for helpful discussion and technical support. This work was supported in part by a Research Grant for Immunology, Allergy and Organ Transplant from the Ministry of Health, Welfare, and Labor of Japan, a Grant-in-Aid for Scientific Research from Japan Society for the Promotion of Science.

References

[1] C. Schick, Y. Kamachi, A.J. Bartuski, S. Cataltepe, N.M. Schechter, P.A. Pemberton, G.A. Silverman, Squamous cell carcinoma antigen 2 is a novel serpin that inhibits the chymotrypsin-like proteinases cathepsin G and mast cell chymase, J. Biol. Chem. 272 (1997) 1849–1855.

[2] S.S. Schneider, C. Schick, K.E. Fish, E. Miller, J.C. Pena, S.D. Treter, S.M. Hui, G.A. Silverman, A serine proteinase inhibitor locus at 18q21.3 contains a tandem duplication of the human squamous cell carcinoma antigen gene, Proc. Natl. Acad. Sci. USA 92 (1995) 3147–3151.

[3] A. Takeda, T. Yamamoto, Y. Nakamura, T. Takahashi, T. Hibino, Squamous cell carcinoma antigen is a potent inhibitor of cysteine proteinase cathepsin L, FEBS Lett. 359 (1995) 78–80.

[4] C. Schick, P.A. Pemberton, G.P. Shi, Y. Kamachi, S. Cataltepe, A.J. Bartuski, E.R. Gornstein, D. Bromme, H.A. Chapman, G.A. Silverman, Cross-class inhibition of the cysteine proteinases cathepsins K, L, and S by the serpin squamous cell carcinoma antigen 1: a kinetic analysis, Biochemistry 37 (1998) 5258–5266.

[5] Y. Sakata, K. Arima, T. Takai, W. Sakurai, K. Masumoto, N. Yuyama, Y. Suminami, F. Kishi, T. Yamashita, T. Kato, H. Ogawa, K. Fujimoto, Y. Matsuo, Y. Sugita, K. Izuhara, The squamous cell carcinoma antigen 2 inhibits the cysteine proteinase activity of a major mite allergen, Der p 1, J. Biol. Chem. 279 (2004) 5081–5087.

[6] N. Yuyama, D.E. Davies, M. Akaiwa, K. Matsui, Y. Hamasaki, Y. Suminami, N. Lu Yoshida, M. Maeda, A. Pandit, J.L. Lordan, Y. Kamogawa, K. Arima, F. Nagumo, M. Sugimachi, A. Berger, I. Richards, S.L. Roberds, T. Yamashita, F. Kishi, H. Kato, K. Arai, K. Ohshima, J. Tadano, N. Hamasaki, S. Miyatake, Y. Sugita, S.T. Holgate, K. Izuhara, Analysis of novel disease-related genes in bronchial asthma, Cytokine 19 (2002) 287–296.

[7] A.J. Bartuski, Y. Kamachi, C. Schick, H. Massa, B.J. Trask, G.A. Silverman, A murine ortholog of the human serpin SCCA2 maps to chromosome 1 and inhibits chymotrypsin-like serine proteinases, Genomics 54 (1998) 297–306.

[8] M. Al-Khunaizi, C.J. Luke, Y.S. Askew, S.C. Pak, D.J. Askew, S. Cataltepe, D. Miller, D.R. Mills, C. Tsu, D. Bromme, J.A. Irving, J.C. Whisstock, G.A. Silverman, The serpin SQN-5 is a dual mechanistic-class inhibitor of serine and cysteine proteinases, Biochemistry 41 (2002) 3189–3199.

[9] D.J. Askew, Y.S. Askew, Y. Kato, R.F. Turner, K. Dewar, J. Lehoczky, G.A. Silverman, Comparative genomic analysis of the clade B serpin cluster at human chromosome 18q21: amplification within the mouse squamous cell carcinoma antigen gene locus, Genomics 84 (2004) 176–184.

[10] K. Masumoto, Y. Sakata, K. Arima, I. Nakao, K. Izuhara, Inhibitory mechanism of a cross-class serpin, the squamous cell carcinoma antigen 1, J. Biol. Chem. 29 (2003) 45296–45304.

[11] T. Takai, R. Mineki, T. Nakazawa, M. Takaoka, H. Yasueda, K. Murayama, K. Okumura, H. Ogawa, Maturation of the activities of recombinant mite allergens Der p 1 and Der f 1, and its implication in the blockade of proteolytic activity, FEBS Lett. 531 (2002) 265–272.

[12] H. Sugihara, S. Toda, N. Yonemitsu, K. Watanabe, Effects of fat cells on keratinocytes and fibroblasts in a reconstructed rat skin model using collagen gel matrix culture, Br. J. Dermatol. 144 (2001) 244–253.

[13] K. Izuhara, T. Heike, T. Otsuka, K. Yamaoka, M. Mayumi, T. Imamura, Y. Niho, N. Harada, Signal transduction pathway of interleukin-4 and interleukin-13 in human B cells derived from X-linked severe combined immunodeficiency patients, J. Biol. Chem. 271 (1996) 619–622.

[14] S. Ye, E.J. Goldsmith, Serpins and other covalent protease inhibitors, Curr. Opin. Struct. Biol. 11 (2001) 740–745.

[15] C. Luke, C. Schick, C. Tsu, J.C. Whisstock, J.A. Irving, D. Bromme, L. Juliano, G.P. Shi, H.A. Chapman, G.A. Silverman, Simple modifications of the serpin reactive site loop convert SCCA2 into a cysteine proteinase inhibitor: a critical role for the P3′ proline in facilitating RSL cleavage, Biochemistry 39 (2000) 7081–7091.

[16] S. Cataltepe, E.R. Gornstein, C. Schick, Y. Kamachi, K. Chatson, J. Fries, G.A. Silverman, M.P. Upton, Co-expression of the squamous cell carcinoma antigens 1 and 2 in normal adult human tissues and squamous cell carcinomas, J. Histochem. Cytochem. 48 (2000) 113–122.

Megakaryocyte proliferation and ploidy regulated by the cytoplasmic tail of glycoprotein Ibα

Taisuke Kanaji, Susan Russell, Janet Cunningham, Kenji Izuhara, Joan E. B. Fox, and Jerry Ware

We have investigated the ability of glycoprotein (GP) Ibα, a megakaryocytic gene product, to sequester the signal transduction protein 14-3-3ξ and to influence megakaryocytopoiesis. Using a Gp1ba$^{-/-}$ mouse colony, we compared the rescued phenotypes produced by a wild-type human GP Ibα allele or a similar allele containing a 6-residue cytoplasmic tail truncation that abrogates binding to 14-3-3ξ. The observed phenotypes illustrate an involvement for GP Ibα in thrombopoietin-mediated events of megakaryocyte proliferation, polyploidization, and the expression of apoptotic markers in maturing megakaryocytes. We developed a hypothesis for the involvement of a GP Ibα/14-3-3ξ/PI-3 kinase complex in regulating thrombopoietin-mediated responses. An observed increase in thrombopoietin-mediated Akt phosphorylation in the truncated variant supported the hypothesis and led to the development of a model in which the GP Ibα cytoplasmic tail sequestered signaling proteins during megakaryocytopoiesis and, as such, became a critical regulator in the temporal sequence of events that led to normal megakaryocyte maturation. (Blood. 2004;104:3161-3168)

Introduction

Megakaryocytopoiesis and thrombopoiesis are highly specialized forms of cell maturation in which bone marrow precursors develop from stem cells, proliferate, and are triggered to differentiate into mature polyploid megakaryocytes.[1,2] A hallmark feature of the process is the repeated endomitotic divisions producing mature megakaryocytes with a DNA content that can reach 128n (diploid = 2n). Subsequent to platelet release, the cytoplasm of the mature megakaryocyte partitions to form a demarcation membrane system, leading to the formation of the platelet precursor, the proplatelet.[3,4] Thrombopoietin (TPO) is the essential cytokine for megakaryocytopoiesis,[5-7] and it stimulates bone marrow precursor cells through a series of signaling pathways, including the Janus kinase/signal transducer and activator of transduction (Jak/STAT), Ras/mitogen-activated protein kinase (Ras/MAPK), and phosphoinositol-3-kinase/Akt (PI3K/Akt) pathways.[8-10] Although the evidence is strong for each of these pathways participating in megakaryocytopoiesis, it is unclear what molecular mechanisms switch a proliferating precursor cell to a path of repeated endomitotic divisions to produce the polyploid megakaryocyte.

A hereditary bleeding disorder, Bernard-Soulier syndrome, is associated with abnormal bone marrow megakaryocytes with a poorly developed demarcation membrane system.[11,12] These abnormal megakaryocytes mimic the presentation of macrothrombocytopenia, characterized by giant circulating platelets and reduced platelet count. The genetic basis of Bernard-Soulier syndrome is well established. It is caused by mutations that impair expression of a multiple subunit receptor, the glycoprotein (GP) Ib-IX complex.[11,13] The molecular basis of macrothrombocytopenia is linked to an absence of the cytoplasmic tail of the GP Ibα subunit of the GP Ib-IX complex.[14] However, a role for the extracytoplasmic domains of the complex cannot be excluded because antibodies to GP Ib-IX can alter proplatelet formation in vitro.[15,16] In addition, in vitro evidence links the expression of GP Ib-IX to cell proliferation, further suggesting the GP Ib-IX complex might regulate megakaryocyte growth.[17]

The mouse phenotype mimicking Bernard-Soulier syndrome in humans can be rescued by expression of a human GP Ibα transgene under the control of a megakaryocytic gene promoter.[11] We have extended this model, generating a comparable mouse colony expressing a variant human GP Ibα subunit lacking the 6 terminal residues (605-610) on the cytoplasmic tail of GP Ibα critical for binding to the signal transduction protein, 14-3-3ξ.[18-21] Using animal models, we tested the hypothesis that sequestering 14-3-3ξ by GP Ibα alters megakaryocytopoiesis and thrombopoiesis. The basis for this hypothesis is the extensive literature on members of the 14-3-3 protein family and their influence in various physiologic processes, including intracellular signaling (Raf, MLK, MEKK, PI3K, IRS-1), cell cycling (Cdc25, Wee1, CDK2, centrosome), apoptosis (BAD, ASK-1), and the regulation of transcription (FKHRL1, DAF-16, p53, TAZ, TLX- 2, histone deacetylase).[22]

Our results identify a link between the GP Ibα/14-3-3ξ interaction and the phosphorylation state of Akt. A model is proposed

From the Department of Molecular and Experimental Medicine, Division of Experimental Hemostasis and Thrombosis, Roon Research Center for Arteriosclerosis and Thrombosis, La Jolla, CA; the Department of Molecular Cardiology, Joseph J. Jacobs Center for Thrombosis and Vascular Biology, The Lerner Research Institute, The Cleveland Clinic Foundation, OH; and the Department of Biomolecular Sciences, Saga Medical School, Japan.

Submitted March 12, 2004; accepted June 27, 2004. Prepublished online as *Blood* First Edition Paper, July 22, 2004; DOI 10.1182/blood-2004-03-0893.

Supported by grants HL50545 and HL31950 (J.W.) and HL30657, HL56264, and HL00903 (J.E.B.F.) from the Heart, Lung and Blood Institute of the National Institutes of Health. The authors are grateful for the support of the Sam and Rose Stein DNA Core Facility within the Department of Molecular and Experimental Medicine at The Scripps Research Institute.

An Inside *Blood* analysis of this article appears in the front of this issue.

Reprints: Jerry Ware, Department of Molecular and Experimental Medicine, Division of Experimental Hemostasis and Thrombosis, Roon Research Center for Arteriosclerosis and Thrombosis, MEM175, 10550 N Torrey Pines Rd, La Jolla, CA 92037; e-mail: jware@uams.edu.

The publication costs of this article were defrayed in part by page charge payment. Therefore, and solely to indicate this fact, this article is hereby marked "advertisement" in accordance with 18 U.S.C. section 1734.

wherein the PI3K/Akt axis of TPO stimulation is regulated by the cytoplasmic tail of GP Ibα during megakaryocyte differentiation. The model is based on results obtained in several different experimental settings, including an in vivo model of severe thrombocytopenia, in vivo administration of TPO, and in vitro analysis of megakaryocyte proliferation and ploidy.

Materials and methods

Generation of mouse models

In vivo use and characterization of a megakaryocyte-specific promoter has been previously described.[23,24] Animals expressing a wild-type human GP Ibα transgene in the absence of mouse GP Ibα [mGp1ba(−/−)–TgN(hGPIbαWT)] and designated, hTg^{WT}, have also been described.[11] Briefly, hTg^{WT} animals were generated by breeding a colony of mice expressing a wild-type human transgene into a GP Ibα knockout mouse colony to produce offspring with heterozygous mouse GP Ibα alleles [mGp1ba(+/−)] and a portion of the offspring expressing the transgene. Expression of the human transgene was established by flow cytometry using the fluorescein isothiocyanate (FITC)–labeled anti–human monoclonal antibody LJ-P3. These mice were again bred to mGp1ba(−/−) mice, and the offspring from this cross were characterized by Southern blot analysis identifying mice lacking 2 mouse GP Ibα alleles and by flow cytometry to identify those expressing the human transgene. These mice are referred to as hTg^{WT} throughout this article. Using a similar breeding strategy, mice expressing a truncated GP Ibα subunit were also generated [mGp1ba(−/−)–TgN(hGPIbαY605X)]. These mice express a human transgene with a stop codon in place of the mature subunit Tyr605 codon (Figure 1). After breeding into the mGp1ba(−/−) mouse colony and selecting animals lacking both mouse GP Ibα alleles, these animals were designated hTg^{Y605X}. Expression of the hTg^{Y605X} transgene is driven by the rat platelet factor 4 promoter, provided by Katya Ravid and Robert Rosenberg (Massachusetts Institute of Technology, Cambridge).[25] The hTg^{Y605X} transgenic construct contained in a 5′ → 3′ direction the rat platelet factor 4 promoter, the coding sequence of human GP Ibα, and the 3′ untranslated cDNA sequence, including the polyadenylation signal sequence. Subsequent expansion of the hTg^{WT} and hTg^{Y605X} colonies was accomplished by breeding into the GP $Ib\alpha^{null}$ colony, a colony that has been backcrossed into the C57/Bl6 strain since its inception. Transgenic animals carrying human GP Ibα alleles have been backcrossed for approximately 6 generations. All animal experiments were performed with approval from the institutional review board of The Scripps Research Institute, La Jolla, CA.

Immunologic reagents

Anti–human GP Ibα monoclonal antibodies LJ-P3 and LJ-Ibα1 were kindly provided by Dr Zaverio Ruggeri (The Scripps Research Institute, La Jolla, CA). Both antibodies recognize the extracytoplasmic domain of platelet GP Ibα.[26] Either denaturation or reduction of human GP Ibα abrogates the epitope of LJ-P3,[27] whereas the LJ-Ibα1 epitope is not sensitive to denaturation and is used for Western blot detection of human GP Ibα antigen. FITC-labeling of purified LJ-P3 was performed according to standard procedures.[28] An antifilamin-1 polyclonal antibody was provided by Drs Hoffmeister and Stossel (Brigham and Women's Hospital, Boston, MA). Other antibodies were purchased from commercial vendors: an FITC-labeled monoclonal antibody recognizing the mouse integrin α_{IIb} subunit was purchased from PharMingen (La Jolla, CA), an anti–14-3-3ζ (C-16) polyclonal antibody was purchased from Santa Cruz Biotechnology (Santa Cruz, CA), an antiphospho-Akt (Ser473) antibody was obtained from New England Biolabs (Beverly, MA), an anti-PI3K polyclonal was purchased from Upstate (Charlottesville, VA), and antiphosphotyrosine polyclonal antibodies (py20 and 4G10) were purchased from Chemicon (Temecula, CA).

von Willebrand factor binding

Using ristocetin (1.5 mg/mL; Sigma, St Louis, MO) as a modulator of von Willebrand factor binding to GP Ib, washed platelets were mixed at a final count of 2×10^8/mL with increasing concentrations of sodium iodide I 125 (^{125}I)–labeled von Willebrand factor (VWF).[23] The mixtures were incubated at 22°C to 25°C for 15 minutes. At the end of the incubation period, platelet-bound VWF and free VWF were separated by centrifuging the

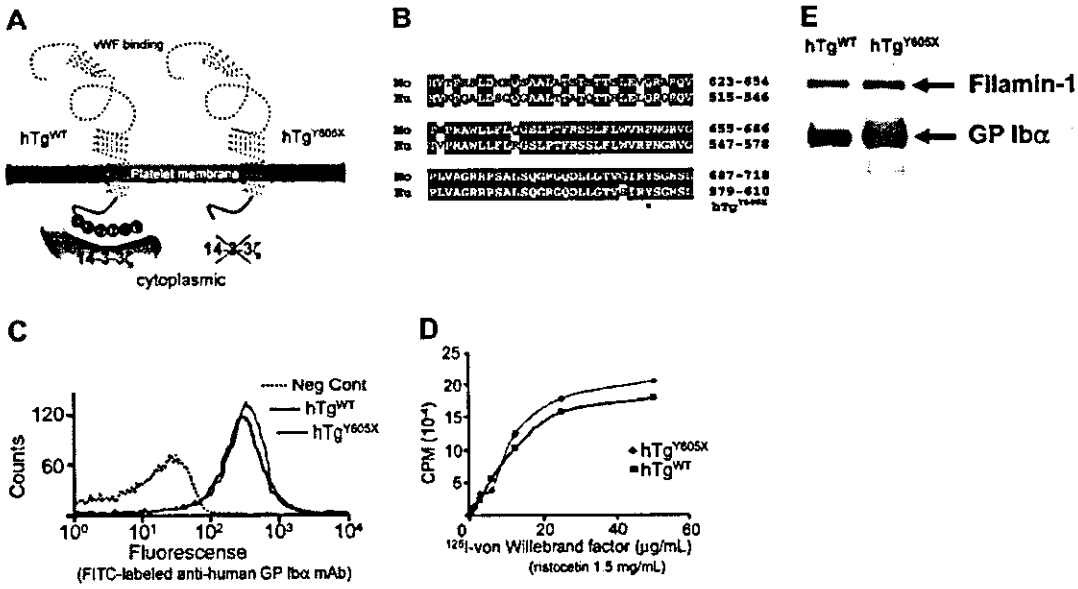

Figure 1. Generation and characterization of mouse models expressing wild-type human GP Ibα (hTg^{WT}) and a truncated form of GP Ibα (hTg^{Y605X}). (A) Animal models have been developed lacking the murine GP Ibα genes and expressing normal human GP Ibα (hTg^{WT}) and a truncated human GP Ibα variant (hTg^{Y605X}). Both expressed human transgenes were driven by megakaryocytic-specific promoters. (B) Shown are the primary sequence alignments for the cytoplasmic tails of mouse (Mo) and human (Hu) GP Ibα. *The amino acid position (605) where a Tyr605 codon was replaced with a stop codon to truncate the cytoplasmic tail of GP Ibα. (C) Flow cytometry profiles of platelets in whole blood are shown using blood from hTg^{WT} and hTg^{Y605X} animals. Fluorescence was produced using an FITC-labeled anti–human GP Ibα monoclonal antibody, LJ-P3. The negative control (dotted line) was fluorescence produced by nontransgenic or normal mice. (D) von Willebrand factor binding isotherms are shown for washed platelets from hTg^{WT} and hTg^{Y605X} blood. (E) Mouse platelet lysates were immunoprecipitated with LJ-P3 and immunoblotted with an antifilamin-1 polyclonal antibody and an anti–GP Ibα polyclonal antibody.

platelets through a sucrose layer, and the platelet-bound radioactivity was measured in a γ-scintillation spectrometer.

Western blot and immunoprecipitation analyses

Platelet pellets prepared from platelet-rich plasma (PRP) were lysed in solubilization buffer (2% Triton X-100, 0.1 M Tris [pH 7.4], 0.01 M EGTA [ethyleneglycotetraacetic acid], 0.15 M NaCl, 2 mM Pefabloc SC [Boehringer Mannheim, Indianapolis, IN]). For sodium dodecyl sulfate–polyacrylamide gel electrophoresis (SDS-PAGE) analysis, the samples were mixed with an SDS sample buffer and were boiled (5 minutes) before electrophoresis. After transfer to nitrocellulose and reactivity with the designated antibodies,[29] the immunoreactive proteins were visualized using a chemiluminescence kit (Amersham Pharmacia Biotech, Piscataway, NJ) and or an iodinated secondary antibody. Immunoreactive signals were identified using Kodak Biomax MR film (Kodak, Rochester, NY).

Immunoprecipitation experiments were performed with washed platelets (3.4×10^8 platelets) resuspended in 250 μL modified Tyrode buffer (137 mM NaCl, 2.7 mM KCl, 2.8 mM dextrose, 0.4 mM NaH_2PO_4, 5 mM HEPES [*N*-2-hydroxyethylpiperazine-*N*′-2-ethanesulfonic acid] [pH 7.4]) and were lysed with an equal volume of solubilization buffer. The mixture was kept on ice for 45 minutes and was centrifuged (10 minutes, 13 000*g*) to remove the insoluble material. Lysates (500 μL) were mixed with 100 μL (50% vol/vol) protein A beads (IPA-300; Repligen, Cambridge, MA) and 10 μg of the indicated antibody for 90 minutes. The beads were then washed 4 times in an equal volume of modified Tyrode buffer and solubilization buffer. Bound proteins were eluted by boiling in SDS-PAGE sample buffer in the presence of 10 mM dithiothreitol.

In vivo model of thrombocytopenia and TPO administration

To induce thrombocytopenia in mice expressing human GP Ibα, 50 μg purified LJ-P3 immunoglobulin G (IgG) was injected into the tail vein of each mouse. Purified recombinant murine TPO was administered subcutaneously (1.5 μg per mouse) to 6- to 8-week-old animals. The TPO was a gift from Dr Hiroshi Miyazaki (Kirin Brewery, Tokyo, Japan). Circulating blood counts were determined using manual methods (Unopette; Becton Dickinson, Franklin Lakes, NJ) and an automated cell counter (Baker, Allentown, PA). The number of platelets and the DNA content of megakaryocytes were analyzed at the indicated time points.

Purification and analysis of mature megakaryocytes

After the induction of thrombocytopenia or the administration of TPO, mice were killed and whole marrow was flushed from both femurs and tibias using a 25-gauge needle until the bone appeared white. Marrow cells are collected in MK buffer (Ca^{2+}, Mg^{2+}-free phosphate-buffered saline [PBS] containing 3% bovine serum albumin [BSA], 5.5 mM D-glucose, 10.2 mM trisodium citrate, and 10 μM prostaglandin E1 [PGE1]) and were filtered through a sterile nylon mesh (70 μm) to remove small bone fragments. Megakaryocytes were harvested by centrifugation (5 minutes, 220*g*) and were overlaid on a discontinuous gradient (0%, 2%, 4%) of BSA. By this method, megakaryocytes made up more than 90% of the cells settling to the bottom within 40 minutes at 1*g*, as evidenced by reactivity with an anti–integrin α_{IIb} monoclonal antibody and acetyl cholinesterase staining.[9]

In vitro culture of murine bone marrow and megakaryocytes

Isolated cells from the bone marrow of mice were suspended at a concentration of 5×10^6 cells/mL in Iscove modified Dulbecco medium (Invitrogen, Carlsbad, CA) supplemented with 20% fetal bovine serum (HyClone, Logan, UT), 1 × Pen/Strep Fungizone Mix (BioWhittaker, Walkersville, MD), and 50 ng/mL murine TPO. Cells were cultured at 37°C in a humidified chamber with 5% CO_2.

Ploidy and TUNEL analysis

DNA ploidy was assessed by flow cytometry. Bone marrow–derived cells were centrifuged (5 minutes, 220*g*) washed, and fixed in 70% ethanol (4°C, overnight). Cells were then washed and resuspended in PBS, incubated for 30 minutes at room temperature with 10 μg/mL FITC-conjugated anti-α_{IIb}, 50 μg/mL propidium iodide (Sigma), and 10 U/mL RNase A (Sigma). Cells were analyzed by flow cytometry using a FACScan (Becton Dickinson). In case of antibody injection, megakaryocytes were enriched before staining using Percoll (Sigma) density centrifugation ($\rho = 1.07$ g/mL) according to the procedure of Tomer et al.[30]

To assay for DNA degradation (TdT-mediated dUTP nick-end labeling [TUNEL] assay), cells were fixed in 1% paraformaldehyde for 15 minutes on ice and were stored in 70% ethanol (−20°C, 30 minutes). This was followed by incubation with terminal deoxynucleotide transferase and fluorescein isothiocyanate-dUTP according to the manual in the APO-Direct Kit (PharMingen).

CFU-Meg assays

For megakaryocyte colony-forming unit (CFU-Meg) assays, bone marrow cells (2×10^5) were cultured with MegaCult-C media (StemCell Technologies, Vancouver, BC, Canada) in the presence of 10 ng/mL recombinant mouse interleukin-3 (IL-3), 20 ng/mL recombinant human IL-6, and 50 ng/mL recombinant mouse TPO (all cytokines courtesy of Kirin Brewery) according to the manufacturer's suggested conditions. After culturing for 7 days, the colonies were stained with acetylcholine esterase, and a CFU-Meg colony was defined as a colony with at least 3 acetylcholine esterase–positive cells.

Platelet preparation and TPO stimulation

Murine blood was withdrawn from the retro-orbital plexus using heparin-coated micro-hematocrit capillaries (Fisher Scientific, Pittsburgh, PA) and was transferred to tubes containing the anticoagulant heparin (Sigma), at a final concentration of 30 U/mL, or acid-citrate-dextrose at a ratio of 1:6. The blood was diluted (1:2) in modified Tyrode buffer, and PRP was prepared by 10-minute centrifugation at 220*g*. PGE1 [10 μM] and apyrase (5 U/mL; Sigma) were added to the PRP. Platelets were washed with 3 sequential centrifugations (2 minutes, 1000*g*) at room temperature. Platelet pellets were washed one additional time with modified Tyrode buffer followed by a final centrifugation (3 minutes, 1000*g*). Final platelet pellets were resuspended in a buffer appropriate for the next procedure, such as immunoprecipitation or Western blot analysis. To analyze the TPO-mediated phosphorylation of Akt, washed platelets were stimulated with TPO (200 ng/mL) at the indicated time points. Phosphorylation was terminated by the addition of an equal volume of 2% SDS, 50 mM Tris-HCl (pH 7.5), 10 mM EGTA, and 2 mM Na_3VO_4.

Results

Murine platelet model with an ablated GP Ibα/14-3-3ξ interaction

Animals devoid of mouse GP Ibα but expressing either of 2 human transgenes were generated to test the hypothesis that a GP Ibα/14-3-3ξ interaction controls aspects of megakaryocyte differentiation. Animals expressing the normal human GP Ibα subunit were designated hTg^{WT}, and those expressing a truncated human GP Ibα subunit were designated hTg^{Y605X} (Figure 1A). The validity of the model was based on a high degree of sequence similarity between human and mouse GP Ibα cytoplasmic domains (Figure 1B) and the ability of human GP Ibα to correct the mouse Bernard-Soulier syndrome.[11] Gross characterization of the hematologic parameters from hTg^{Y605X} animals, including platelet count and platelet size, gave results indistinguishable from those obtained using platelets from hTg^{WT} animals.[11] Tail bleeding time assays, crude measurements of mouse hemostasis and coagulation, were also comparable between the 2 colonies of mice and were indistinguishable from those of healthy mice (data not shown).

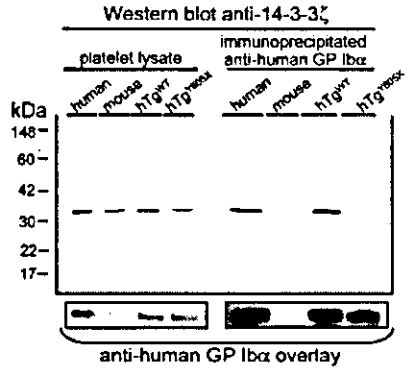

Figure 2. Truncation of platelet GP Ibα at Tyr605 ablates the interaction between GP Ibα and 14-3-3ξ. (Left) Western blot of platelet lysates detecting 14-3-3ξ protein at approximately 32 kDa in human platelets, mouse platelets, and mouse platelets expressing human GP Ibα subunits but devoid of mouse GP Ibα (hTg^{WT} and hTg^{Y605X}). The experiment demonstrated that total levels of 14-3-3ξ were similar in each of the samples. (Right) Results obtained after immunoprecipitation of human GP Ibα. Bound anti–14-3-3ξ antibody was detected using radiolabeled goat anti–rabbit IgG. Results demonstrate that the truncation of GP Ibα ablated the interaction with 14-3-3ξ, as evidenced by the lack of 14-3-3ξ antigen. Longer exposures of the autoradiograph failed to detect any 14-3-3ξ antigen in the hTg^{Y605X} sample. The same nitrocellulose filter was probed a second time with an anti–human GP Ibα monoclonal antibody, LJ-Ibα1, and demonstrated the presence of GP Ibα antigen in those samples in which the human subunit was present (bottom panel).

Critical for a comparison of the hTg^{WT} and hTg^{Y605X} transgenic megakaryocytes or platelets was the level of expressed human antigen. Using a monoclonal antibody that recognized a conformation-specific epitope within the amino terminus of GP Ibα, the expression levels produced by both transgenes were virtually indistinguishable (Figure 1C). Binding isotherms using the radiolabeled ligand, VWF, produced similar binding to hTg^{WT} and hTg^{Y605X} platelets (Figure 1D). The similar levels of GP Ibα antigen expressed by hTg^{WT} and hTg^{Y605X} reflected the rate-limiting requirement of GP Ibα and GP IX to assemble the multiple subunit GP Ib-IX complex.[31,32] Intracytoplasmic levels of GP Ibα antigen were higher in platelet lysates from hTg^{Y605X} animals (Figure 1E), even though the surface-expressed levels were similar. In addition, we observed similar levels of filamin-1 associated with each cytoplasmic tail, further validating structural integrity (Figure 1E). Thus, 2 mouse colonies were established expressing similar levels of human GP Ibα antigen and differing only in their cytoplasmic tail lengths.

Next we performed immunoprecipitation experiments using an anti–human GP Ibα monoclonal antibody to determine in vivo whether an absence of the 6-terminal residues of GP Ibα residues would lead to loss of interaction with 14-3-3ξ. Indeed, 14-3-3ξ was coimmunoprecipitated from mouse platelets expressing the wild-type human GP Ibα, whereas immunoprecipitation of the truncated GP Ibα molecule failed to copurify 14-3-3ξ, even though comparable levels of human GP Ibα antigen were immunoprecipitated (Figure 2).

Truncation of GP Ibα altered megakaryocyte ploidy in an acute model of severe thrombocytopenia

An anti–human GP Ibα mouse monoclonal antibody, LJ-P3, recognized an amino terminal extracytoplasmic domain of human GP Ibα and reacted with platelets from hTg^{WT} and hTg^{Y605X} animals (Figure 1C). When the intact IgG of LJ-P3 was injected into the tail veins of mice expressing human GP Ibα, it produced severe thrombocytopenia; circulating platelet counts dropped to 3% to 5% of normal level within 24 hours of injection (Figure 3A). The requirement of human GP Ibα and LJ-P3 to produce thrombocytopenia was evident by the failure of the antibody to produce any thrombocytopenia in nontransgenic animals (Figure 3A). After injections of LJ-P3 into hTg^{WT} animals, platelet counts started to increase after approximately 7 days (Figure 3A). In contrast, when LJ-P3 was injected into hTg^{Y605X} animals, platelet counts recovered more quickly, with a return to 50% of normal platelet count 4 days after antibody injection (Figure 3A).

To determine whether the platelet count recovery in the 2 animal models coincided with changes in bone marrow megakaryocytes, we examined megakaryocyte ploidy before and after antibody-induced thrombocytopenia. Before antibody injection, the megakaryocyte ploidy profiles were indistinguishable in hTg^{WT} and hTg^{Y605X} marrow (Figure 3B). In addition, the steady-state number of megakaryocytes was the same in the 2 colonies, as determined by the number of α_{IIb}-positive cells identified by flow cytometry of bone marrow aspirates (not shown). However, by day 4 after antibody-induced thrombocytopenia, the marrow from hTg^{Y605X} animals contained an increased percentage of megakaryocytes, with a ploidy of 32n or greater (Figure 3B). hTg^{WT} bone marrow by day 4 contained an increased percentage of 16n megakaryocytes. During the recovery from thrombocytopenia, the percentage of megakaryocytes in an 8n or less ploidy class was indistinguishable in the hTg^{WT} and the hTg^{Y605X} marrow (Figure 3B).

Truncation of GP Ibα alters the in vivo megakaryocytic response to TPO

Results from antibody-induced thrombocytopenia suggested a link between the cytoplasmic tail of GP Ibα and megakaryocytopoiesis. We further examined this possibility by testing the hypothesis that TPO-mediated proliferation of megakaryocytes differs in the 2 GP Ibα murine models. First, we injected hTg^{WT} mice and hTg^{Y605X}

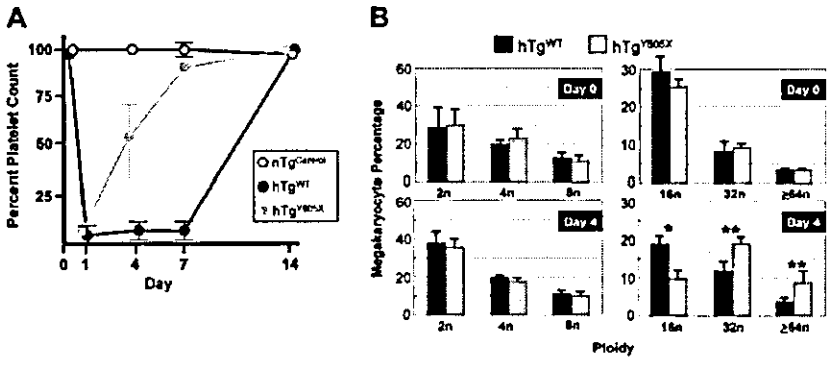

Figure 3. Acute model of severe thrombocytopenia. (A) The anti–human GP Ibα mouse monoclonal antibody, LJ-P3, injected into the tail veins of mice expressing human GP Ibα, produced severe thrombocytopenia. When injected into mice expressing the wild-type human GP Ibα subunit (hTg^{WT}), the platelet count started to return to a normal level after day 7. In mice expressing a truncated form of GP Ibα (hTg^{Y605X}), the platelet count began to recover by day 4, and by day 7 the platelet counts were near normal levels. A control LJ-P3 injection into nontransgenic mice ($nTg^{Control}$) is shown for comparison. (B) The ploidy profile of megakaryocytes is shown before injection of the anti–human monoclonal antibody, LJ-P3 (day 0) and 4 days after injection (day 4). Results were compiled from individual mice, and the mean and SEM are shown (n = 6). *P = .01; **P = .05.

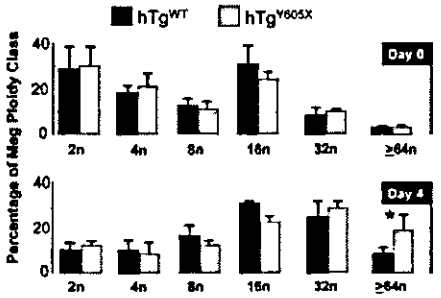

Figure 4. Ploidy analysis of bone marrow megakaryocytes after in vivo administration of TPO. After the injection of TPO, bone marrow megakaryocytes were harvested and analyzed for ploidy classes. Shown are the means and SEM from 6 mice of each genotype. *P = .05.

mice with equivalent amounts of TPO. A single subcutaneous injection of TPO (1.5 μg) caused a similar increase in platelet count in both models at days 2, 4, and 6, with a 3-fold increase over baseline as the maximum level of response (not shown). Next, we examined the effects of TPO on megakaryocyte ploidy. At 4 days after TPO injection, the extent of polyploidization was again different in the 2 models (Figure 4). Megakaryocytes of a high ploidy class, 64n or greater; were significantly increased in the marrow of hTg^{Y605X} animals, whereas the lower ploidy classes were indistinguishable (Figure 4).

Truncation of GP Ibα alters megakaryocytic proliferation and markers of apoptosis

Megakaryocytes from both animal models were tested in vitro for their proliferative potential and the ability to express terminal differentiation markers. CFU-Mk assays revealed no difference in the number of megakaryocytic progenitor cells for each model (hTg^{WT} = 13.8 ± 5.4; hTg^{Y605X} = 15.0 ± 3.9). However, after in vitro culturing for 5 days in the presence of TPO, hTg^{WT} cultures were enriched in megakaryocytes, as evidenced by a 2-fold increase in acetyl cholinesterase–positive cells when compared with similar cultures from hTg^{Y605X} marrow (Table 1; Figure 5A). Similar to the in vivo results presented in Figure 5, the culture of hTg^{Y605X} bone marrow produced an increase in the percentage of higher ploidy cells (not shown). Thus, the number of progenitor cells in each model was similar in the marrow, but the hTg^{WT} cells had a greater proliferative potential whereas the hTg^{Y605X} marrow produced megakaryocytes with higher ploidy content.

Next, we considered whether the hTg^{Y605X} cells containing an increased percentage of high ploidy cells might also express increased levels of terminal differentiation markers. TUNEL assays were performed to monitor apoptosis as a function of DNA degradation. After 5 days the in vitro culture of hTg^{Y605X} bone marrow produced megakaryocytes with a higher occurrence of apoptosis (Figure 5B), a difference no longer apparent by day 8 of culture (not shown). Further evidence for the changes in the hTg^{Y605X} megakaryocyte population was apparent by the increased accumulation of GP Ibα antigen (Figure 5C). An increase in GP Ibα expression also supported the more differentiated state of the hTg^{Y605X} megakaryocytes after stimulation with TPO. Thus, the truncation of the GP Ibα tail limited the proliferative potential of megakaryocytic precursors (Table 1) while increasing their intrinsic ability to progress through a sequence of events leading to the presence of late-stage megakaryocytes.

Table 1. In vitro bone marrow cultures

	Total no. cells, × 10^7		No. megakaryocytes, × 10^4	
Day	hTg^{WT}	hTg^{Y605X}	hTg^{WT}	hTg^{Y605X}
0	7.71 ± 0.65	7.57 ± 0.99	—	—
5	1.48 ± 0.17	1.44 ± 0.57	13.67 ± 1.58	7.54 ± 1.34

n = 4.
– indicates undetectable.

Truncation of GP Ibα leads to increased phosphorylation of Akt

To explain the results observed in in vivo and in vitro assays, we considered the possibility that the PI3K/Akt axis of TPO stimulation is altered in the hTg^{Y605X} model.[9] A physical link is reported among 14-3-3ξ, PI3K, and GP Ibα,[33] and the relevance of PI3K for TPO stimulation of megakaryocytes is well documented.[9,34] Our hypothesis suggested that ablation of the 14-3-3ξ interaction between GP Ibα and 14-3-3ξ has altered one of the major stimulatory pathways for megakaryocytopoiesis, the PI3K activation of Akt.[9]

To address this problem and to determine how much PI3K was associated with GP Ibα, we stimulated human platelets with TPO, immunoprecipitated with either an anti–GP Ibα antibody or an

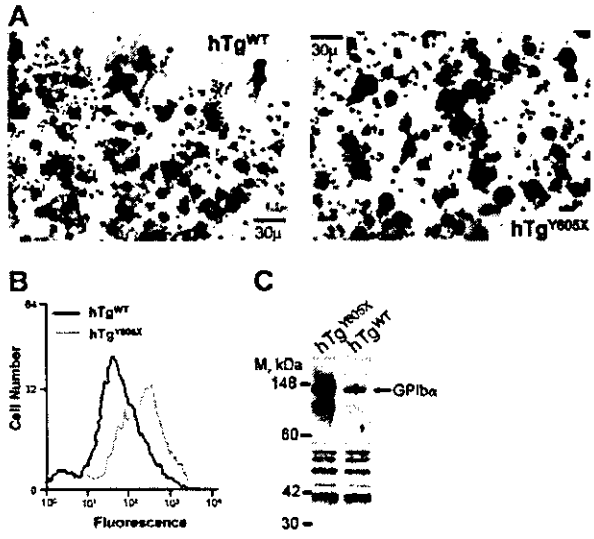

Figure 5. In vitro analysis of cultured bone marrow cells. (A) Shown are images from the cultured bone marrow preparations illustrating the increased proliferation of hTg^{WT} cells compared with hTg^{Y605X} cells (for comparison, see also Table 1). Images were captured with an Olympus IX71 inverted microscope equipped with a 40 ×/0.95 NA objective (Olympus, Tokyo, Japan). Images were photographed at 400 × original magnification with an Olympus DP70 CCD camera (Olympus) and acquired through Lumina Vision software (Mitani, Fukui, Japan). Cells were stained for acetylcholinesterase using 0.1 mol/L PBS containing 0.05% acetylthiocholine iodide, 0.1 mol/L sodium citrate, 30 mmol/L copper sulfate, and 5 mmol/L potasium ferricyanide (pH 6.0). (B) TUNEL assay on cultured bone marrow cells. Bone marrow cells were harvested and cultured for 5 days in the presence of TPO, and TUNEL assays were performed. Flow cytometry settings were used to gate and provide data for cells with greater than 4n ploidy. (C) Western blot from the same cultures depicted in the center panel was blotted for GP Ibα antigen, a marker of late-stage megakaryocytopoiesis. Ten micrograms protein (BCA assay) was applied to each lane, electrophoresed, transferred to nitrocellulose, and reacted with an anti–GP Ibα antibody. Shown is the resultant autoradiograph. Samples from hTg^{Y605X} show an increase in the amount of GP Ibα antigen compared with hTg^{WT}, consistent with an increase in high-ploidy cells seen after a 5-day culture in the presence of TPO. However, as seen in Figures 1 and 2, gene expression levels for both transgenes were similar, but coincident with an increase in the percentage of high-ploidy megakaryocytes was an increase in GP Ibα antigen. The blot was subsequently reprobed with a pool of antibodies to confirm a similar protein load and is shown below for comparison.

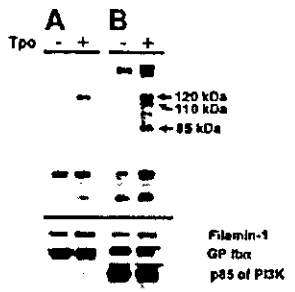

Figure 6. TPO-induced phosphorylation. Purified human platelets were stimulated with TPO (200 ng/mL, 10 minutes, 37°C) and were immunoprecipitated with an anti–GP Ibα monoclonal (LJ-P3) (A) or an anti-PI3K antibody (B). Immunoprecipitation products were electrophoresed and blotted with an antiphosphotyrosine antibody (4G10). Phosphorylated proteins in the absence (-) or presence (+) of TPO are shown. Subsequent control blots were performed on the same filter for filamin-1, GP Ibα, and the p85 subunit of PI3K.

anti-PI3K antibody. We blotted the immunoprecipitated material with an antiphosphotyrosine antibody (4G10) and looked for links among GP Ibα, PI3K, and c-Mpl. Figure 6A shows a protein (120 kDa) that became increasingly phosphorylated in the presence of TPO and immunoprecipitated by an anti–GP Ibα antibody. As shown in the accompanying control, PI3K was immunoprecipitated by the anti–GP Ibα monoclonal antibody, but a phosphorylated form of the protein was not detected. A protein of similar mobility (120 kDa) was also immunoprecipitated by an anti-PI3K antibody along with major phosphorylated proteins of 110 and 85 kDa (Figure 6B). Thus, a 120-kDa protein appeared to be immunoprecipitated by anti-PI3K and anti–GP Ibα antibodies after stimulation with TPO. The results also illustrate that only a minor portion of PI3K is associated with GP Ibα. These results suggest that a complex exists of GP Ibα, PI3K, and an unidentified 120-kDa protein and that several of these proteins become phosphorylated in the presence of TPO.

If the phosphorylation state of PI3K is relevant to the differences we observed between the hTg^{WT} and hTg^{Y605X} colonies, we would expect to observe further downstream consequences, such as the phosphorylation of a PI3K target, Akt. We examined the TPO-induced phosphorylation of Akt in platelets from both models and found a heightened Akt phosphorylation in hTg^{Y605X} platelets (Figure 7A). In contrast, the overall phosphorylation pattern observed with an antiphosphotyrosine antibody revealed no dramatic differences in the 2 colonies (Figure 7B). These results confirm a shift in the PI3K/Akt pathway and establish an involvement of the GP Ibα/PI3K/14-3-3ξ interaction in the regulation of this signaling pathway.

Discussion

The presented results are consistent with a model in which the cytoplasmic tail of GP Ibα influences the temporal sequence of events necessary for the proliferation and maturation of megakaryocyte progenitors. Our hypothesis began with 14-3-3ξ and its sequestering by GP Ibα as a regulator of megakaryocytopoiesis. The sequestration of 14-3-3ξ by GP Ibα has implications for platelet function by down-regulating the activation of Cdc42 and Rac.[35] Because our model with ablated interaction between GP Ibα and 14-3-3ξ displayed changes in megakaryocyte ploidy, we were led to consider the contributions of the major regulator of megakaryocyte development, TPO.[6,7] The relevance of TPO to our results was evident by a decreased in vitro proliferation potential of hTg^{Y605X} megakaryocytic stem cells (Table 1) and an increased percentage of high ploidy hTg^{Y605X} cells (Figure 4). Of the TPO activation pathways, the PI3K/Akt pathway seemed to be the most likely involved because both the TPO receptor and the GP Ibα/14-3-3ξ complex sequester PI3K.[34,36] Indeed, in the absence of a GP Ibα/14-3-3ξ interaction, an increased phosphorylation of Akt in response to TPO was observed (Figures 7, 8A). Thus, the TPO response in megakaryocytes can be influenced by membrane receptors other than c-mpl, just as platelet activation can be primed by TPO and by the activation of a PI3K-dependent pathway.[37]

Although the target of activated Akt could be any number of proteins, activated Akt increases the posttranslational stability of cyclins.[38] Cyclins are particularly relevant targets because they have been associated with promoting the endomitosis that leads to increased ploidy.[39] Cyclin D3 is active in promoting passage through the G_1 phase of mitosis,[40] and its importance as a megakaryocytic gene product has been established.[39,41] In addition, the overexpression of D1 or D3 cyclin in transgenic animals increases megakaryocyte ploidy.[42,43] Phenotypically, the overexpression of D3 impairs formation of the mature megakaryocyte demarcation membrane system,[43] similar to what occurs with a complete absence of a GP Ib-IX complex.[11,12] Thus, the abnormal megakaryocyte cytoplasm associated with Bernard-Soulier syndrome may reflect an unregulated activation of cyclins in the absence of GP Ib-IX or, in the current study, by a short truncation in the cytoplasmic tail. Together, these results illustrate the requirement for a highly coordinated temporal sequence of events leading to the formation of a developing platelet field in the cytoplasm of a normal megakaryocyte.

Our results demonstrate increases in Akt phosphorylation and in markers of apoptosis (Figure 5B). This seems to be in direct conflict with the dogma establishing the PI3K/Akt pathway as a cell survival or

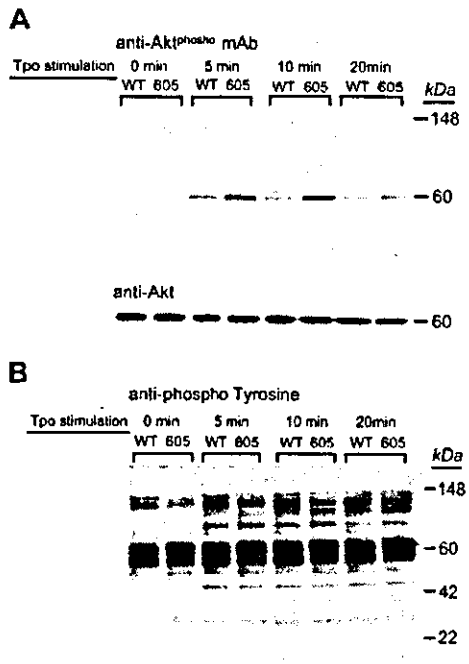

Figure 7. TPO-induced Akt phosphorylation. Purified platelets from hTg^{WT} and hTg^{Y605X} were stimulated with TPO (200 ng/mL) for the indicated times. Platelet lysates were subjected to Western blot analysis using either an antiphospho-Akt (Ser473) antibody (A) or an antiphosphotyrosine polyclonal antibody (B). The upper blot was reprobed using an anti-Akt polyclonal antibody to visualize protein loads and is shown for comparison (middle panel).

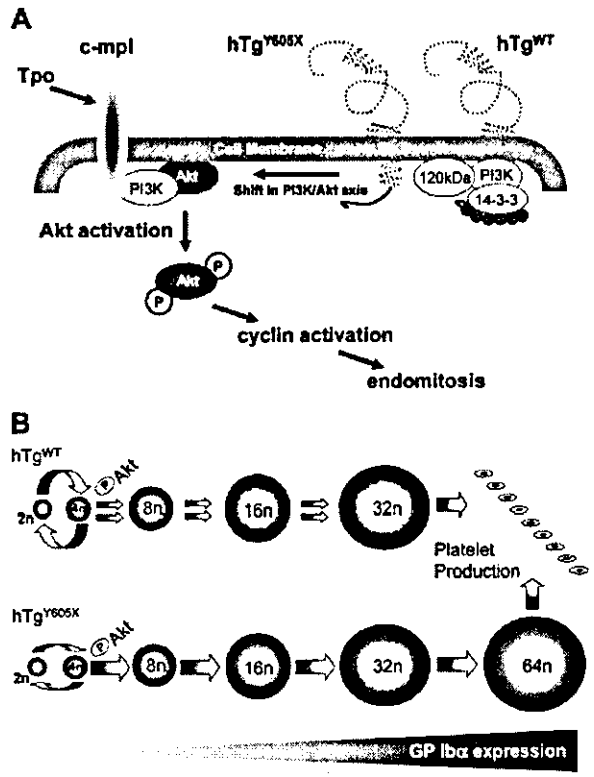

Figure 8. GP Ibα expression, megakaryocyte proliferation, and differentiation. (A) Results suggest a shift in the PI3K/Akt axis of TPO stimulation. A hypothesis is presented whereby the cytoplasmic tail of GP Ibα sequesters signaling proteins, such as 14-3-3ξ and PI3K, and down-regulates the Akt-dependent pathway. In the truncated GP Ibα variant, hTg^{Y605X}, a shift in the PI3K/Akt axis results in increased Akt activation and downstream consequences of increased endomitosis and accumulation of a greater percentage of high-ploidy megakaryocytes. (B) A schematic model is presented to illustrate how an increase in Akt phosphorylation results in a megakaryocyte population with increased ploidy. The precursor cell proliferation (2n → 4n → 2n) is more active in the hTg^{WT} model (Table 1) and is depicted by larger arrows compared with proliferation in the hTg^{Y605X} model. However, Akt phosphorylation in response to TPO is increased in the hTg^{Y605X} model (Figure 6A) and corresponds to an increase in the accumulation of cells of higher ploidy (Figures 3B, 4). Thus, repeated endomitotic divisions in the hTg^{Y605X} marrow are depicted by larger arrows compared with a similar process in the hTg^{WT} model. The increased proliferative potential of hTg^{WT} cells and the potential for hTg^{Y605X} cells to generate megakaryocytes of a higher ploidy class provide mechanisms whereby both models produce similar levels of platelet. Results highlight the independence of ploidy and platelet release in response to stimuli. GP Ibα expression increases during megakaryocyte maturation and, as such, becomes a critical timing factor for normal megakaryocyte maturation.

an antiapoptotic pathway.[44] Exceptions do exist, however, and they reflect the downstream targets of the activated Akt.[45] Worth considering are the unique properties of the megakaryocyte. Increased apoptotic markers are not a deleterious result of maturation but are part of the normal physiology of the megakaryocyte proceeding along the pathway to maturation. Clearly, the PI3K/Akt pathway is crucial to a wide range of processes in the multicellular organism, and our results underscore the inability to identify a single unifying theme for activation through a PI3K/Akt pathway.

Originally, we believed the faster platelet recovery observed in the hTg^{Y605X} model (Figure 3) could be a consequence of the increased percentage of megakaryocytes of higher ploidy. However, this conclusion did not fit when we observed the in vivo administration of TPO-altered megakaryocyte ploidy in the 2 models without altering the rate of increase in the circulating platelet count. Thus, by what mechanism does antibody-induced thrombocytopenia occur, and, more important, what explains the different platelet recovery rates in the 2 animal models? We present data showing that the expressed levels of transgene on the platelet surface and within platelet lysates were similar in both animal models (Figure 1C-E). The levels of megakaryocytic GP Ibα were also similar before the induction of thrombocytopenia (not shown). However, the levels of GP Ibα antigen changed dramatically when the megakaryocytic population changed, as seen in Figure 5C. The mechanism of antibody-induced thrombocytopenia could have existed at several points. First, it could have had a direct effect on proplatelet production in the marrow. This would be analogous to the in vitro inhibition described by others.[15,16] As such, proplatelet formation by megakaryocytes with increased GP Ibα antigen would be less inhibited, as would have occurred within the hTg^{Y605X} marrow after the induction of thrombocytopenia (Figure 3B). The net result would be an increased rate of circulating platelet recovery in the hTg^{Y605X} animal. Second, the antibody would have a direct effect on the circulating platelets. It is possible that by unlinking GP Ibα with 14-3-3ξ, we altered the clearance kinetics of the platelets in each model. In this case, the antibody produced a difference in platelet count that had nothing to do with the state of the megakaryocyte within the marrow.

In further support of the idea that the different platelet recovery rates observed in antibody-induced thrombocytopenia might be irrelevant to megakaryocyte proliferation and maturation, we observed that in vivo administration of TPO increased the hTg^{Y605X} ploidy (Figure 4) but did not increase the rate of platelet release. We suggest the similar increases in platelet count are explained by a level of compensation dependent on the increased cell proliferation in the hTg^{WT} model (Table 1) balanced by the higher ploidy in the hTg^{Y605X} marrow (Figure 8B). In support of this idea is the similar percentage of α_{IIb}-positive cells 4 days after TPO administration (2.50 ± 0.6 for hTg^{WT} vs 2.66 ± 0.08 for hTg^{Y605X}; $n = 6$). These results highlight an independence of ploidy and platelet release in the megakaryocyte population.[2,7,46]

One noticeable aspect of the presented results is the requirement for a stressed system to identify differences between the hTg^{WT} and the hTg^{Y605X} genotypes. The normal megakaryocyte ploidy profile and the circulating platelet counts are indistinguishable in the 2 models. However, changes are seen after induced severe thrombocytopenia or after in vivo administration of TPO. These results highlight the potential for compensation among signaling pathways in the unstressed situation. Indeed, the ability of hematopoietic cells to compensate in the absence of specific proteins or signaling pathways is not without precedence, and it highlights the complexity of normal hematopoiesis.[47-49]

In summary, we have found a mechanism by which the cytoplasmic tail of GP Ibα can modulate megakaryocyte ploidy and proliferation. The involved pathways most likely represent one defect contributing to the generation of the macrothrombocytopenic phenotype typical of Bernard-Soulier syndrome. Our results also identify factors capable of regulating the commitment of a normal megakaryocyte to become a polyploid cell. GP Ibα expression increases during megakaryocytic differentiation.[50] but the low levels of GP Ibα expression during early megakaryocytopoiesis may influence the level of Akt phosphorylation and balance the proliferative potential of a precursor cell compared with the cell's commitment to a pathway of repeated endomitotic cycles. Our results illustrate a temporal sequencing of events that control the commitment of the megakaryocyte to undergo endomitosis. Expressed levels of GP Ibα and sequestration of signaling proteins become relevant in controlling the mechanisms associated with megakaryocytopoiesis and thrombopoiesis.

References

1. Gewirtz AM. Megakaryocytopoiesis: the state of the art. Thromb Haemost. 1995;74:204-209.
2. Ravid K, Lu J, Zimmet JM, Jones MR. Roads to polyploidy: the megakaryocyte example. J Cell Physiol. 2002;190:7-20.
3. Zucker-Franklin D, Kaushansky K. Effect of thrombopoietin on the development of megakaryocytes and platelets: an ultrastructural analysis. Blood. 1996;88:1632-1638.
4. Italiano JE, Lecine P, Shivdasani RA, Hartwig JH. Blood platelets are assembled principally at the ends of proplatelet processes produced by differentiated megakaryocytes. J Cell Biol. 1999;147: 1299-1312.
5. de Sauvage FJ, Carver-Moore K, Luoh SM, et al. Physiological regulation of early and late stages of megakaryocytopoiesis by thrombopoietin. J Exp Med. 1996;183:651-656.
6. Kaushansky K. Thrombopoietin: understanding and manipulating platelet production. Annu Rev Med. 1997;48:1-11.
7. Zimmet J, Ravid K. Polyploidy: occurrence in nature, mechanisms, and significance for the megakaryocyte-platelet system. Exp Hematol. 2000;28:3-16.
8. Drachman JG, Rojnuckarin P, Kaushansky K. Thrombopoietin signal transduction: studies from cell lines and primary cells. Methods. 1999;17: 238-249.
9. Geddis AE, Fox NE, Kaushansky K. Phosphatidylinositol 3-kinase is necessary but not sufficient for thrombopoietin-induced proliferation in engineered Mpl-bearing cell lines as well as in primary megakaryocytic progenitors. J Biol Chem. 2001;276:34473-34479.
10. Matsumura I, Kanakura Y. Molecular control of megakaryocytopoiesis and thrombopoiesis. Int J Hematol. 2002;75:473-483.
11. Ware J, Russell S, Ruggeri ZM. Generation and rescue of a murine model of platelet dysfunction: the Bernard-Soulier syndrome. Proc Natl Acad Sci U S A. 2000;97:2803-2808.
12. Poujol C, Ware J, Nieswandt B, Nurden AT, Nurden P. Absence of GP Ibα is responsible for the aberrant membrane development during megakaryocyte differentiation: ultrastructural study using a transgenic model. Exp Hematol. 2002;30:352-360.
13. Lopez JA, Andrews RK, Afshar-Kharghan V, Berndt MC. Bernard-Soulier syndrome. Blood. 1998;91:4397-4418.
14. Kanaji T, Russell S, Ware J. Amelioration of the macrothrombocytopenia associated with the murine Bernard-Soulier syndrome. Blood. 2002;100: 2102-2107.
15. Takahashi R, Sekine N, Nakatake T. Influence of monoclonal antiplatelet glycoprotein antibodies on in vitro human megakaryocyte colony formation and proplatelet formation. Blood. 1999;93: 1951-1958.
16. Alimardani G, Guichard J, Fichelson S, Cramer EM. Pathogenic effects of anti-glycoprotein Ib antibodies on megakaryocytes and platelets. Thromb Haemost. 2002;88:1039-1046.
17. Feng S, Christodoulides N, Kroll MH. The glycoprotein Ib/IX complex regulates cell proliferation. Blood. 1999;93:4256-4263.
18. Gu M, Xi X, Englund GD, Berndt MC, Du X. Analysis of the roles of 14-3-3 in the platelet glycoprotein Ib-IX-mediated activation of integrin $\alpha_{IIb}\beta_3$ using a reconstituted mammalian cell expression model. J Cell Biol. 1999;147:1085-1096.
19. Zaffran Y, Meyer SC, Negrescu E, Reddy KB, Fox JEB. Signaling across the platelet adhesion receptor glycoprotein Ib-IX induces $\alpha_{IIb}\beta_3$ activation both in platelets and a transfected Chinese hamster ovary cell system. J Biol Chem. 2000;275: 16779-16787.
20. Feng S, Christodoulides N, Reséndiz JC, Berndt MC, Kroll MH. Cytoplasmic domains of GpIbα and GpIbβ regulate 14-3-3ζ binding to GpIb/IX/V. Blood. 2000;95:551-557.
21. Dong JF, Li CQ, Saetung G, et al. The cytoplasmic domain of glycoprotein (GP) Ibα constrains the lateral diffusion of the GP Ib-IX complex and modulates von Willebrand factor binding. Biochemistry. 1997;36:12421-12427.
22. Fu H, Subramanian RR, Masters SC. 14-3-3 proteins: structure, function and regulation. Annu Rev Pharmacol Toxicol. 2000;40:617-647.
23. Ware J, Russell SR, Marchese P, Ruggeri ZM. Expression of human platelet glycoprotein Ibα in transgenic mice. J Biol Chem. 1993;268:8376-8382.
24. Fujita H, Hashimoto Y, Russell S, Zieger B, Ware J. In vivo expression of murine platelet glycoprotein Ibα. Blood. 1998;92:488-495.
25. Ravid K, Beeler DL, Rabin MS, Ruley HE, Rosenberg RD. Selective targeting of gene products with the megakaryocyte platelet factor 4 promoter. Proc Natl Acad Sci U S A. 1991;88:1521-1525.
26. Handa M, Titani K, Holland LZ, Roberts JR, Ruggeri ZM. The von Willebrand factor-binding domain of platelet membrane glycoprotein Ib: characterization by monoclonal antibodies and partial amino acid sequence analysis of proteolytic fragments. J Biol Chem. 1986;261:12579-12585.
27. Murata M, Ware J, Ruggeri ZM. Site-directed mutagenesis of a soluble recombinant fragment of platelet glycoprotein Ibα demonstrating negatively charged residues involved in von Willebrand factor binding. J Biol Chem. 1991;266: 15474-15480.
28. Harlow E, Lane D. Labeling antibodies. In: Antibodies: A Laboratory Manual. Cold Spring Harbor, NY: Cold Spring Harbor Laboratory; 1988:319-358.
29. Harlow E, Lane D. Antibodies: A Laboratory manual. Cold Spring Harbor, NY: Cold Spring Harbor Laboratory; 1988.
30. Tomer A, Harker LA, Burstein SA. Purification of human megakaryocytes by fluorescence-activated cell sorting. Blood. 1987;70:1735-1742.
31. Dong JF, Gao S, Lopez JA. Synthesis, assembly, and intracellular transport of the platelet glycoprotein Ib-IX-V complex. J Biol Chem. 1998;273: 31449-31454.
32. Strassel C, Pasquet JM, Alessi MC, et al. A novel missense mutation shows that GPIbβ has a dual role in controlling the processing and stability of the platelet GPIb-IX adhesion receptor. Biochemistry. 2003;42:4452-4462.
33. Munday AD, Berndt MC, Mitchell CA. Phosphoinositide 3-kinase forms a complex with platelet membrane glycoprotein Ib-IX-V complex and 14-3-3ζ. Blood. 2000;96:577-584.
34. Miyakawa Y, Rojnuckarin P, Habib T, Kaushansky K. Thrombopoietin induces phosphoinositol 3-kinase activation through SHP2, Gab, and insulin receptor substrate proteins in BAF3 cells and primary murine megakaryocytes. J Biol Chem. 2001;276:2494-2502.
35. Bialkowska K, Zaffran Y, Meyer SC, Fox JE. 14-3-3ζ mediates integrin-induced activation of Cdc42 and Rac: platelet glycoprotein Ib-IX regulates integrin-induced signaling by sequestering 14-3-3ζ. J Biol Chem. 2003;278:33342-33350.
36. Wu Y, Asazuma N, Satoh K, et al. Interaction between von Willebrand factor and glycoprotein Ib activates Src kinase in human platelets: role of phosphoinositide 3-kinase. Blood. 2003;101: 3469-3476.
37. Pasquet JM, Gross BS, Gratacap MP, et al. Thrombopoietin potentiates collagen receptor signaling in platelets through a phosphatidylinositol 3-kinase–dependent pathway. Blood. 2000;95: 3429-3434.
38. Chang F, Lee JT, Navolanic PM, et al. Involvement of PI3K/Akt pathway in cell cycle progression, apoptosis, and neoplastic transformation: a target for cancer chemotherapy. Leukemia. 2003; 17:590-603.
39. Wang Z, Zhang Y, Kamen D, Lees E, Ravid K. Cyclin D3 is essential for megakaryocytopoiesis. Blood. 1995;86:3783-3788.
40. Matsushime H, Quelle DE, Shurtleff SA, et al. D-type cyclin-dependent kinase activity in mammalian cells. Mol Cell Biol. 1994;14:2066-2076.
41. Wang Z, Zhang Y, Lu J, Sun S, Ravid K. Mpl ligand enhances the transcription of the cyclin D3 gene: a potential role for Sp1 transcription factor. Blood. 1999;93:4208-4221.
42. Sun S, Zimmet JM, Toselli P, et al. Overexpression of cyclin D1 moderately increases ploidy in megakaryocytes. Haematologica. 2001;86:17-23.
43. Zimmet JM, Ladd D, Jackson CW, Stenberg PE, Ravid K. A role for cyclin D3 in the endomitotic cell cycle. Mol Cell Biol. 1997;17:7248-7259.
44. Hunter T. Signaling—2000 and beyond. Cell. 2000;100:113-127.
45. Chen HK, Fernandez-Funez P, Acevedo SF, et al. Interaction of Akt-phosphorylated ataxin-1 with 14-3-3 mediates neurodegeneration in spinocerebellar ataxia type 1. Cell. 2003;113:457-468.
46. Ebbe S. Biology of megakaryocytes. Prog Hemost Thromb. 1976;3:211-229.
47. Semerad CL, Poursine-Laurent J, Liu F, Link DC. A role for G-CSF receptor signaling in the regulation of hematopoietic cell function but not lineage commitment or differentiation. Immunity. 1999;11: 153-161.
48. Lorenz M, Slaughter HS, Wescott DM, et al. Cyclooxygenase-2 is essential for normal recovery from 5-fluorouracil-induced myelotoxicity in mice. Exp Hematol. 1999;27:1494-1502.
49. Zhou Q, Zhao J, Wiedmer T, Sims PJ. Normal hemostasis but defective hematopoietic response to growth factors in mice deficient in phospholipid scramblase 1. Blood. 2002;99:4030-4038.
50. Lepage A, Leboeuf M, Cazenave JP, et al. The $\alpha_{IIb}\beta_3$ integrin and GPIb-V-IX complex identify distinct stages in the maturation of CD34(+) cord blood cells to megakaryocytes. Blood. 2000;96: 4169-4177.

THE JOURNAL OF BIOLOGICAL CHEMISTRY
Vol. 279, No. 7, Issue of February 13, pp. 5081–5087, 2004
Printed in U.S.A.

The Squamous Cell Carcinoma Antigen 2 Inhibits the Cysteine Proteinase Activity of a Major Mite Allergen, Der p 1*

Received for publication, October 22, 2003, and in revised form, November 6, 2003
Published, JBC Papers in Press, November 20, 2003, DOI 10.1074/jbc.M311585200

Yasuhisa Sakata,[a] Kazuhiko Arima,[a] Toshiro Takai,[b] Wataru Sakurai,[c] Kiyonari Masumoto,[a] Noriko Yuyama,[d] Yoshinori Suminami,[e] Fumio Kishi,[f] Tetsuji Yamashita,[g] Takeshi Kato,[b] Hideoki Ogawa,[b] Kazuma Fujimoto,[h] Yo Matsuo,[c] Yuji Sugita,[d] and Kenji Izuhara[a,i,j]

From the [a]Division of Medical Biochemistry, Department of Biomolecular Sciences, the [b]Division of Gastroenterology, Department of Internal Medicine, and the [i]Division of Medical Research, Center for Comprehensive Community Medicine, Saga Medical School, Saga, 849-8501, the [h]Atopy (Allergy) Research Center, Juntendo University, Tokyo, 113-8421, the [c]Computational Proteomics Team, Protein Research Group, RIKEN Genomic Sciences Center, Yokohama, 230-0045, [d]Genox Research, Inc., Tokyo, 112-8088, [e]Onoda Municipal Hospital, Onoda, 756-0094, the [f]Department of Microbiology and Immunology, Kagoshima University Dental School, Kagoshima, 890-8544, and [g]Mitsubishi-Kagaku BCL, Tokyo, 174-8555, Japan

The squamous cell carcinoma antigens 1 (SCCA1) and SCCA2 belong to the ovalbumin-serpin family. Although SCCA1 and SCCA2 are closely homologous, these two molecules have distinct properties; SCCA1 inhibits cysteine proteinases such as cathepsin K, L, and S, whereas SCCA2 inhibits serine proteinases such as cathepsin G and human mast cell chymase. Although several intrinsic target proteinases for SCCA1 and SCCA2 have been found, the biological roles of SCCA1 and SCCA2 remain unknown. A mite allergen, Der p 1, is one of the most immunodominant allergens and also acts as a cysteine proteinase probably involved in the pathogenesis of allergic diseases. We have recently shown that both SCCA1 and SCCA2 are induced by two related Th2-type cytokines, IL-4 and IL-13, in bronchial epithelial cells and that SCCA expression is augmented in bronchial asthma patients. In this study, we explored the possibility that SCCA proteins target Der p 1, and it turned out that SCCA2, but not SCCA1, inhibited the catalytic activities of Der p 1. We furthermore analyzed the inhibitory mechanism of SCCA2 on Der p 1. SCCA2 contributed the suicide substrate-like mechanism without formation of a covalent complex, causing irreversible impairment of the catalytic activity of Der p 1, as SCCA1 does on papain. In addition, resistance to cleavage by Der p 1 also contributed to the inhibitory mechanism of SCCA2. These results suggest that SCCA2 acts as a cross-class serpin targeting an extrinsic cysteine proteinase derived from house dust mites and that it may have a protective role against biological reactions caused by mites.

The squamous cell carcinoma antigens 1 (SCCA1: SERPINB3)[1] and SCCA2 (SERPINB4) belong to the ovalbumin-serpin (serine proteinase inhibitors) family and are 91% identical at the amino acid level (1). Both genes locate at 18q21.3 very closely, suggesting that either gene could arise from the other by gene duplication (2). SCCA1 was originally purified from squamous cell carcinoma of uterine cervix (3), and it turned out that SCCA1 and SCCA2 are co-expressed broadly in normal tissues: the epithelium of tongue, tonsil, esophagus, uterine cervix, vagina, and the conducting airways; Hassall's corpuscles of the thymus; and some areas of the skin (4). Although SCCA1 and SCCA2 are very homologous, these two molecules have distinct properties; SCCA1 inhibits cysteine proteinases such as cathepsin K, L, S, and papain, whereas SCCA2 inhibits serine proteinases such as cathepsin G and human mast cell chymase (1, 5, 6). The specificities of SCCA1 and SCCA2 are due to the difference in the reactive site loop (RSL) sequences because only 7 amino acid residues among 13 (54%) were identical in the RSL regions (P7 to P6') of these proteins (7). Although target proteinases for most serpins are the chymotrypsin family, the serpin inhibiting cysteine proteinases is defined as a cross-class inhibitor. Cytokine response modifier A (CrmA) derived from cowpox virus and proteinase inhibitor 9 (PI9, SERPINB9) inhibits both a serine proteinase (granzyme B) and a cysteine proteinase (caspase proteins) (8–11). So thus far, SCCA1, CrmA, and PI9 are all obvious cross-class serpins (12). Although several intrinsic target proteinases for SCCA1 and SCCA2 have been found, the biological roles of SCCA1 and SCCA2 remain unknown. We have recently shown that expression of both SCCA1 and SCCA2 is up-regulated by two related Th2-type cytokines, IL-4 and IL-13, in bronchial epithelial cells and that SCCA expression is augmented in bronchial lesions and in peripheral blood of bronchial asthma patients (13). It is well known that IL-4 and IL-13 are involved in the pathogenesis of bronchial asthma (14, 15), predominantly expressed in the lesions of asthma patients (16–18). These findings raise the possibility that SCCA1 and SCCA2 may perform their activities in the lesions of bronchial asthma.

Der p 1 and Der f 1, group I allergens derived from house dust mites, *Dermatophagoides pteronyssinus* and *Dermatophagoides farinae*, respectively, are major components of mites (10–20%), and their presence is closely correlated with development of bronchial asthma, atopic dermatitis, and allergic rhinitis (19–22). It has been reported that more than half of anti-mite allergen antibodies and 10–20% of total IgE in aller-

* This work was supported in part by a Research Grant for Immunology, Allergy and Organ Transplant from the Ministry of Health, Welfare, and Labor of Japan and a grant-in-aid for Scientific Research from the Japan Society for the Promotion of Science. The costs of publication of this article were defrayed in part by the payment of page charges. This article must therefore be hereby marked "*advertisement*" in accordance with 18 U.S.C. Section 1734 solely to indicate this fact.

[j] To whom correspondence should be addressed. Tel.: 81-952-34-2261; Fax: 81-952-34-2058; E-mail: kizuhara@med.saga-u.ac.jp.

[1] The abbreviations used are: SCCA, squamous cell carcinoma antigen; RSL, reactive site loop; CrmA, cytokine response modifier A, PI9, proteinase inhibitor 9; PAR-2, protease-activated receptor 2; MALDI-TOF, matrix-associated laser desorption ionization time-of-flight; PEO-M, polyethylene oxide-maleimide.

TABLE I
Comparison of k_{cat} and K_m for BSA-treated and SCCA2-treated Der p 1

	k_{cat}	K_m	k_{cat}/K_m
	s^{-1}	μM	s^{-1}/M^{-1}
BSA-treated (n = 3)	0.444 ± 0.0173	248 ± 16.2	1790 ± 46.3
SCCA2-treated (n = 3)	0.0155 ± 0.00260	290 ± 71.0	54.2 ± 4.40[a]

[a] Statistically significant difference *versus* BSA-treated at p = 0.0000003.

gic patients are anti-Der p 1 antibodies, which indicates that Der p 1 is one of the most immunodominant allergens (19, 21). Der p 1 is a 25-kDa cysteine proteinase; its amino acid sequence conserves 3 critical amino acids (Cys-34, His-170, and Asn-190) comprising the catalytic triad as other cysteine proteinases (23). The structure of Der p 1 has been modeled based on the crystal structure of papain, suggesting that Der p 1 is composed of two domains separated by a cleft, where the active site with the catalytic triad locates (24). It has been reported that Der p 1 cleaves several proteins such as occludin (25), protease-activated receptor 2 (PAR-2) (26), CD23 (27), CD25 (28), and CD40 (29) *in vitro*. Although the precise role of the catalytic activity of Der p 1 *in vivo* has not been elucidated, the following results indicate that the catalytic activity of Der p 1 would be important for the pathogenesis of bronchial asthma, in addition to its antigenicity. 1) Der p 1 disrupts tight junctions by cleaving occludin, increasing the permeability of the bronchial epithelial barrier (25). 2) Der p 1 causes secretion of inflammatory cytokines such as IL-6, IL-8, granulocyte-macrophage colony-stimulating factor, and RANTES in bronchial epithelial cells by activating PAR-2 (26, 30, 31). 3) Der p 1 induces the Th2 subset by cleaving CD25 on T cells (28) or CD40 on dendritic cells (29).

We hypothesized that SCCA proteins induced by IL-4 and IL-13 target extrinsic proteinases derived from house mites in the lesions of bronchial asthma. To explore this possibility, we examined whether SCCA1 and SCCA2 inhibit the catalytic activities of group I mite allergens in this study. It turned out that SCCA2 inhibited the catalytic activities of both Der p 1 and Der f 1 and that SCCA2 performed its inhibitory activity by irreversibly impairing the catalytic activity of Der p 1 and by being resistant to the cleavage by Der p 1. These results suggest that SCCA2 acts as a cross-class serpin targeting extrinsic cysteine proteinases, Der p 1 and Der f 1, and that SCCA2 may have a protective role against mite-caused biological reactions.

EXPERIMENTAL PROCEDURES

Materials—Papain, E-64, cathepsin G, cathepsin L, and human mast cell chymase were purchased from Sigma, Peptide Institute Inc. (Osaka, Japan), Calbiochem, Athens Research & Technology (Athens, GA), and Cortex Biochem (San Leandro, CA), respectively.

Generation of Plasmids and Recombinant Proteins—SERPINB3 and *SERPINB4* cDNA incorporated into pGEX(-KG)-4T (Amersham Biosciences) were prepared as reported before (32). SCCA2 mutants were generated by oligonucleotide-directed mutagenesis using two complemented primers with mutations. Standard PCR amplification was performed using the SCCA2 cDNA as a template and a mixture of primers. DNA fragments with mutations were ligated into pGEX-KG-SCCA2 plasmid. The RSL-replaced mutants of SCCA1 and SCCA2 were similarly generated by digestion and ligation into the StuI/XbaI site of them.

GST-fused SCCA1 and SCCA2 proteins were expressed in an *Escherichia coli* strain, BL21, and isolated by using glutathione-Sepharose 4B beads (Amersham Biosciences). Purity of the generated proteins was greater than 95%, as estimated by Coomasie staining of an SDS-PAGE gel. Concentrations of the proteins were determined by Protein Assay (Bio-Rad).

Generation of the Der p 1 and Der f 1 Protein—Recombinant Der p 1 and Der f 1 proteins were generated as described before (33, 34). Briefly, proforms of four recombinant house dust mite group 1 allergens, Der p 1-N52Q, Der p 1-WT, Der f 1-N53Q, and Der f 1-WT, were secreted into the culture supernatant of transfectant cells of *Pichia pastoris* and converted to the mature forms with prosequences removed by dialysis against an acidic buffer. The mature forms were purified with anion exchange column chromatography. The purity was more than 95%, as estimated by SDS-PAGE. The protein concentration was determined by Protein Assay. Der p 1-N52Q and Der f 1-N53Q were used for most experiments.

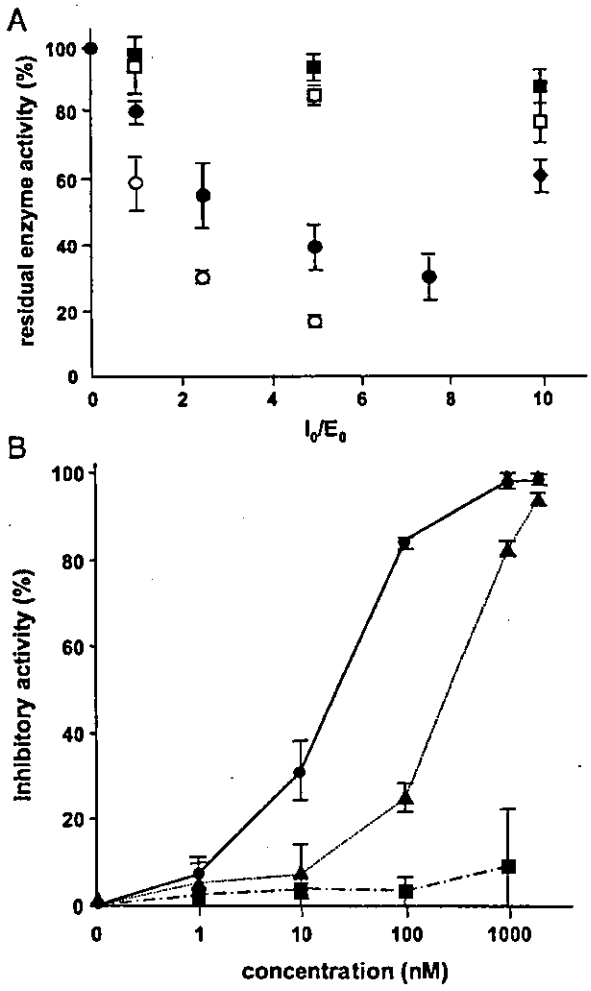

FIG. 1. **Inhibitory effects of SCCA molecules on the catalytic activities of group I house mite allergens.** In *A*, SCCA1 (*square*) or SCCA2 (*circle*) or E-64 (*rhombus*) was incubated with 10 nM preactivated Der p 1 (*closed*) or Der f 1 (*open*) at the indicated I_0/E_0 ratio for 30 min at 25 °C. Residual enzyme activities are depicted. In *B*, SCCA1 (*closed triangles*) or SCCA2 (*closed circles*) or GST alone (*closed squares*) was incubated with the indicated concentrations of preactivated Der p 1 at the I_0/E_0 ratio = 1 for 30 min at 25 °C. Inhibitory activities are depicted.

Enzyme Assays—Enzyme assays of Der p 1 and Der f 1 were performed as described before (33, 35). The substrate used for enzyme assays was butyloxycarbonyl-Gln-Arg-methylcoumarin (Boc-Gln-Ala-Arg-MCA), purchased from Peptide Institute Inc. The indicated concentrations of Der p 1 or Der f 1 preactivated with 2 mM dithiothreitol for 10 min at 25 °C were incubated with the indicated concentrations of GST-fused SCCA proteins for 30 min at 25 °C in activity-measuring buffer (50 mM sodium phosphate, pH 7.0, 1 mM EDTA, 2 mM dithiothre-

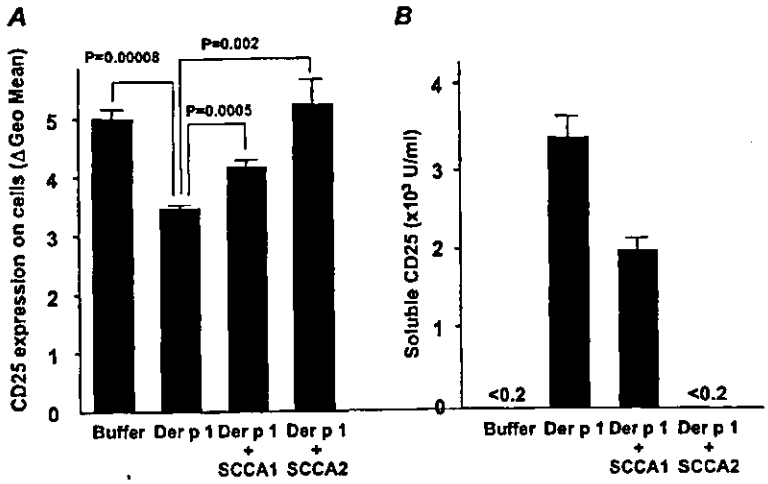

FIG. 2. **Inhibitory effects of SCCA molecules on the cleavage of CD25 by Der p 1.** One μM SCCA1 or SCCA2 was incubated with 2 μM preactivated Der p 1 for 30 min at 25 °C. Then, stimulated Jurkat T cells were incubated with a mixture of Der p 1 and SCCA proteins with final concentrations 0.6 and 0.3 μM, respectively, for 2 h at 37 °C. Expression of CD25 on the cell surface (*A*) and amount of soluble CD25 (*B*) are depicted.

itol, and 0.001% BSA). Upon addition of 100 μM substrate to the reaction mixture, the residual enzyme activity was measured by continuous monitoring, using excitation and emission wavelengths of 380 and 460 nm, respectively.

Cleavage Assay of CD25—Procedures of cleavage assay of CD25 were performed as described before (28). A human acute T cell leukemia cell line, Jurkat T cells, was stimulated with 100 nM PMA (Sigma) and 1 μM ionomycin (Sigma) for 30 h in RPMI 1640 medium containing 10% fetal calf serum followed by suspension with serum-free AIM V medium (Invitrogen). Two μM Der p 1 preactivated with 2 mM dithiothreitol was incubated with 1 μM SCCA proteins for 30 min at 25 °C. Then, CD25 cleavage was performed by incubating Jurkat cells with the mixture of Der p 1 and SCCA proteins with the final concentrations of Der p 1 and SCCA proteins 0.6 and 0.3 μM, respectively, for 2 h at 37 °C. Expression of CD25 on cell surface was analyzed by flow cytometry using anti-CD25 antibody (Beckman Coulter), and soluble CD25 in the supernatant was immunoassayed in the Mitsubishi Kagaku BCL laboratories by means of a commercial kit.

Matrix-associated Laser Desorption Ionization Time-of-Flight (MALDI-TOF) Mass Spectrometry—Five μM Der p 1 and 10 μM SCCA proteins were mixed in phosphate reaction buffer for 2 h at 4 °C, and then the reactive samples were applied to Voyager RP MALDI-TOF mass spectrometry (PerSeptive Biosystems, Framingham, MA).

Separation of the Incubated SCCA Proteins and Der p 1—After 2 μM Der p 1 and SCCA proteins were incubated in phosphate reaction buffer for 30 min at 25 °C, the reaction mixture was applied to the high pressure liquid chromatography system equipped with ProteinPak 300SW (Waters, Milford, MA). Then, the subjected samples were eluted with phosphate buffer (50 mM sodium phosphate, pH 7.0), and each fraction was subjected to SDS-PAGE or the enzyme assay. The gels were stained with silver using 2D-SILVER STAIN II "Daiichi" (Daiichi Pure Chemicals, Tokyo, Japan). The quantities of the proteins on the gels were determined by SYPRO Ruby staining (Molecular Probes, Eugene, OR)

Chemical Modification of the Cysteine Residues of Der p 1—The fractionated Der p 1 was incubated with 0.4 mM EZ-Link PEO-maleimide activated biotin ((+)-biotinyl-3-maleimidopropiomamidyl-3, 6-dioxaoctanediamine; PEO-M-biotin, Pierce) for 2 h at 25 °C. The samples were applied to SDS-PAGE and then transferred to polyvinylidene difluoride membranes. The membranes were blotted with horseradish peroxidase-conjugated streptavidin (Zymed Laboratories Inc., South San Francisco, CA).

Synthesized Peptides—Synthesized peptides used for inhibition assays were Thr-Ala-Val-Val-Gly-Phe-Gly-Ser-Ser-Pro-Thr-Ser-Thr (SCCA1-13 mer), Thr-Ala-Val-Val-Val-Val-Glu-Leu-Ser-Ser-Pro-Ser-Thr (SCCA2-13 mer), and Thr-Ala-Val-Val-Val-Val-Gly-Leu-Ser-Pro-Thr-Ser-Thr (SCCA2 tm-13 mer), all purchased from Peptide Institute Inc. The peptides were dissolved in dimethyl sulfoxide (Wako, Osaka, Japan).

RESULTS

Expression and Purification of Functional SCCA1 and SCCA2—To perform functional analyses of SCCA1 and SCCA2, we expressed and purified recombinant proteins of GST-fused SCCA1 and SCCA2. We confirmed that SCCA1

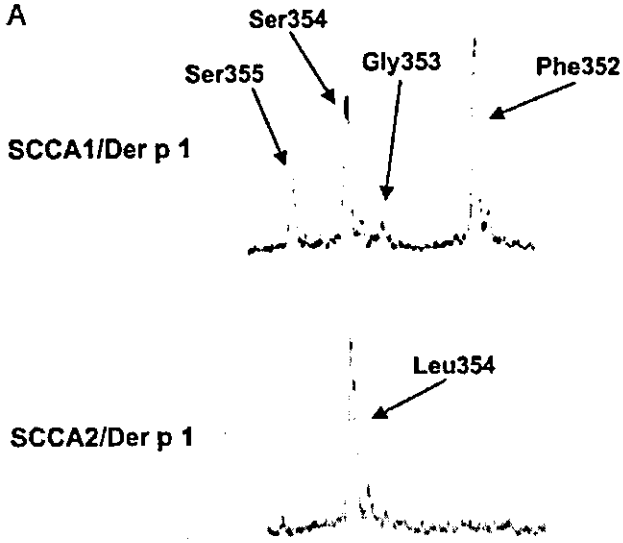

FIG. 3. **Identification of the cleaved sites of SCCA molecules by Der p 1.** Ten μM SCCA1 or SCCA2 and 5 μM Der p 1 were incubated for 2 h at 4 °C, and the reactive samples were applied to MALDI-TOF mass spectrometry. The detected peaks (*A*) and the identified cleavage sites (*B*) are depicted. The *arrows* represent the peptides from the indicated residues to the C terminus (*A*).

inhibited the cysteine protease activities of papain and cathepsin L but not the serine protease activities of cathepsin G and human mast cell chymase, whereas SCCA2 showed the opposite effects, as reported previously (32). These results demonstrated that purified SCCA1 and SCCA2 proteins were functional.

Inhibition of Catalytic Activities of Der p 1 and Der f 1 by SCCA2—We first analyzed whether SCCA1 or SCCA2 inhibited catalytic activities of Der p 1 and Der f 1. The k_{cat} and K_m values of Der p 1 used in the experiments were estimated as 0.444 ± 0.0173 s^{-1} and 248 ± 16.2 μM, respectively (Table I). An irreversible inhibitor for cysteine proteinase, E-64, displayed only 39% of inhibition at a 10:1 ratio at 10 nM Der p 1 or

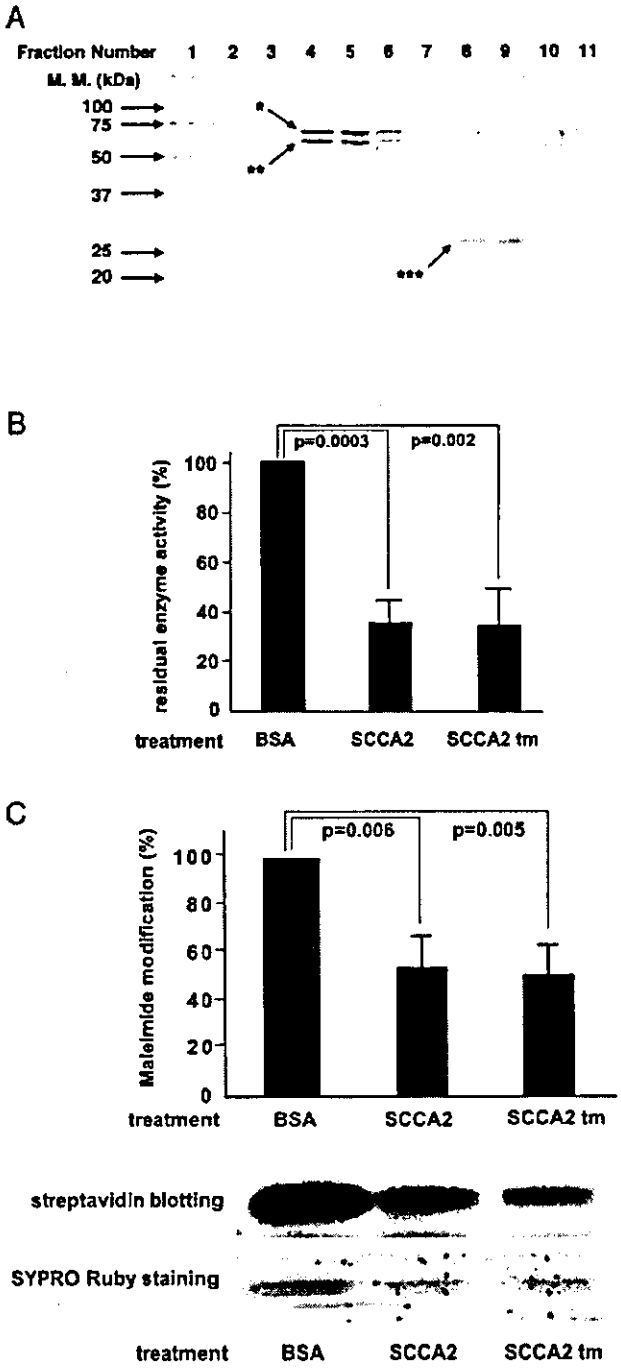

FIG. 4. **Elution profile of the mixture of SCCA molecules and Der p 1 by gel-filtration column and the catalytic activity of SCCA-treated Der p 1.** Two μM SCCA proteins was incubated with 2 μM preactivated Der p 1. In *A*, the samples incubated for 30 min were applied to the gel-filtration column. Elution profiles stained with silver are depicted. The *arrows* represent the intact (*) and truncated (**) SCCA2 and Der p 1 (***), respectively. *M. M.*, molecular mass. In *B*, the catalytic activities of the fractionated Der p 1 in the presence of SCCA2 or BSA are depicted. In *C*, fractionated Der p 1 in the presence of SCCA2 or BSA was incubated with PEO-M-biotin followed by blotting with horseradish peroxidase-conjugated streptavidin or was stained by SYPRO Ruby. The incorporation of PEO-M-biotin and their representative data are depicted.

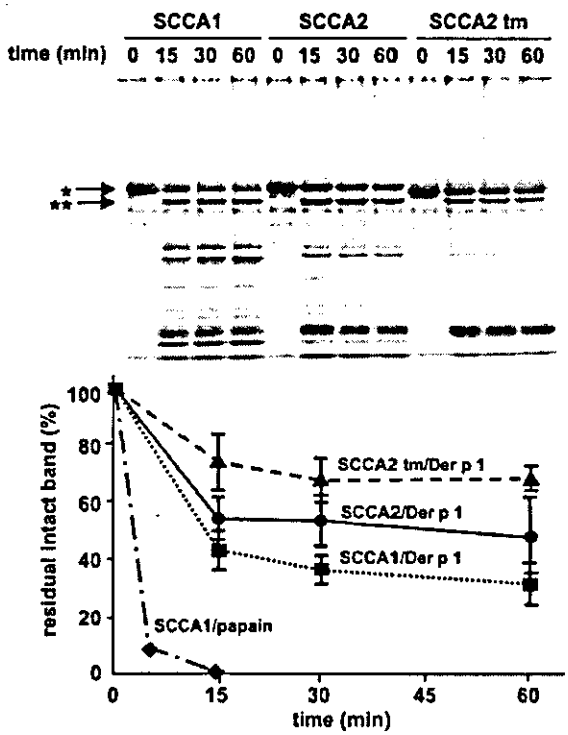

FIG. 5. **Cleavage profile of SCCA molecules by Der p 1.** SCCA2 proteins were incubated with Der p 1 or papain, as shown in Fig. 4. The samples incubated for the indicated times followed by SYPRO Ruby staining and the amounts of intact SCCA proteins at the indicated time are plotted. The *arrows* represent the intact (*) and truncated (**) SCCA proteins.

Der f 1 (Fig. 1*A*). Therefore, active site titration of Der p 1 or Der f 1 was impossible, so we analyzed dose-dependent effects of SCCA1 and SCCA2 on the catalytic activity of Der p 1 and Der f 1. When the concentration of Der p 1 or Der f 1 was fixed at 10 nM, SCCA2 inhibited catalytic activities of both Der p 1 and Der f 1 in a dose-dependent manner, whereas SCCA1 showed only 10% inhibition at 10:1 ratio (Fig. 1*A*). The inhibitory effects of SCCA2 were independent of glycosylation of Der p 1 and Der f 1 (data not shown). When the ratio of Der p 1 and SCCA1 or SCCA2 was fixed at 1:1, the inhibitory effect of SCCA2 increased dependent of the concentration, reaching almost 100% at 1 μM (Fig. 1*B*). SCCA1 showed a weaker inhibitory effect when compared with SCCA2. GST alone had no inhibitory effect. These results demonstrated that SCCA2, and to a lesser extent SCCA1, targeted Der p 1 and that SCCA2 is a cross-class serpin that can inhibit both serine and cysteine proteinases as well as CrmA, PI9, and SCCA1.

Inhibitory Effects of SCCA Proteins on CD25 Cleavage by Der p 1—To examine whether SCCA2 shows its inhibitory effect on Der p 1, when Der p 1 targets not only the synthetic peptide, but also an intact protein as a substrate, we analyzed the inhibitory effects of SCCA proteins on CD25 cleavage by Der p 1. Incubation of Der p 1 with activated Jurkat cells caused the cleavage of CD25 (Fig. 2*A*, 31 ± 2.0%, n = 3). The presence of SCCA2 completely restored expression of CD25, and so did SCCA1 to some extent. Furthermore, existence of the soluble CD25 in the supernatant was observed in parallel with the cleavage of CD25 on Jurkat cells (Fig. 2*B*). These results meant that SCCA2 also exerts its inhibitory effects on the interaction of Der p 1 with CD25.

Determination of the Cleavage Sites in SCCA1 and SCCA2 by Der p 1—We next identified the cleavage sites in RSLs of SCCA1 and SCCA2 by Der p 1, using MALDI-TOF mass spectrometry. Analysis of Der p 1-cleaved peptides in SCCA1 by MALDI-TOF mass spectrometry showed the existence of four

TABLE II
Alignment of RSLs of SCCA proteins and their inhibitory activities

Position	Proximal hinge							Reactive site loop												Distal hinge	Inhibition
	14	13	12	11	10	9	8	7	6	5	4	3	2	1	1′	2′	3′	4′	5′	6′	11′	
SCCA2	G	V	E	A	A	A	A	T	A	V	V	V	V	E	L	S	S	P	S	T	C	+
SCCA1	·	A	·	·	·	·	·	·	·	·	·	G	F	G	S	·	P	T	·	·	H	−
SCCA2 RSL1	·	A	·	·	·	·	·	·	·	·	·	G	F	G	S	·	P	T	·	·	H	−
SCCA1 RSL2	·	·	·	·	·	·	·	·	·	·	·	·	·	·	·	·	·	·	·	·	·	+
SCCA2 mut1 (V351G)	·	·	·	·	·	·	·	·	·	·	·	G	·	·	·	·	·	·	·	·	·	−
SCCA2 mut2 (V352F)	·	·	·	·	·	·	·	·	·	·	·	·	F	·	·	·	·	·	·	·	·	−
SCCA2 mut4 (L354S)	·	·	·	·	·	·	·	·	·	·	·	·	·	·	S	·	·	·	·	·	·	−
SCCA2 mut3 (E353G)	·	·	·	·	·	·	·	·	·	·	·	·	·	G	·	·	·	·	·	·	·	++
SCCA2 E353A	·	·	·	·	·	·	·	·	·	·	·	·	·	A	·	·	·	·	·	·	·	++
SCCA2 E353Q	·	·	·	·	·	·	·	·	·	·	·	·	·	Q	·	·	·	·	·	·	·	++
SCCA2 mut5 (S356P, P357T)	·	·	·	·	·	·	·	·	·	·	·	·	·	·	·	·	P	T	·	·	·	++
SCCA2 tm (E353G, S356P, P357T)	·	·	·	·	·	·	·	·	·	·	·	·	·	G	·	·	P	T	·	·	·	++++
SCCA2 tm P356A	·	·	·	·	·	·	·	·	·	·	·	·	·	G	·	·	A	T	·	·	·	++++

[a] ·, the same amino acid as SCCA2.

peaks corresponding to the peptides from Phe-352, Gly-353, Ser-354, and Ser-355 to the C terminus, whereas the analyses with SCCA2 displayed only one peak, corresponding to the peptide from Leu-354 to the C terminus (Fig. 3). These results indicated that Der p 1 would interact with SCCA2 firmly, generating a serpin-proteinase complex as other serpins do. In contrast, the interaction between Der p 1 and SCCA1 would not be tight, and Der p 1 would cleave non-specifically the RSL of SCCA1.

Non-covalent Binding of SCCA2 with Der p 1—Although it is well known that a serpin and its target proteinase form an acyl-enzyme intermediate linked by an oxy-ester bond, stable for hydrolysis (36), we have recently demonstrated that SCCA1 inhibited the catalytic activity of papain without forming a covalent bond (32). We next analyzed the association manner of SCCA2 and Der p 1. To retain the native association between SCCA2 and Der p 1, we employed a gel-filtration system. We used a mixture of Der p 1 and SCCA2 in which the catalytic activity of Der p 1 was completely inhibited. Subsequently, SCCA2 and Der p 1 were eluted according to their molecular masses (Fig. 4*A*). These results demonstrated that SCCA2 interacted with Der p 1 by non-covalent binding as well as the interaction between SCCA1 and papain.

Irreversible Inhibition of Der p 1 by SCCA2 Treatment—We next investigated how SCCA2 inhibited the catalytic activity of Der p 1 without forming a covalently bound complex. To study the effects of the interaction between SCCA2 and Der p 1, we analyzed the catalytic activity of the SCCA2-treated Der p 1 eluted by the gel-filtration column. Although the catalytic activity of Der p 1 was completely inhibited in the solution containing 2 μM Der p 1 and SCCA2, which was applied to the column, it turned out that the catalytic activity of fractionated Der p 1 decreased, but still existed, when compared with the solution before fractionation (36 ± 9.4%, n = 3, Fig. 4*B*). The k_{cat}/K_m value of SCCA2-treated Der p 1 was significantly less than that of BSA-treated Der p 1 (54.2 ± 4.40 *versus* 1790 ± 46.3 s^{-1} M^{-1}, p = 0.0000003, Table I), which confirmed the impairment of the catalytic activity.

These results raised the possibility that SCCA2 treatment caused a conformational change of Der p 1, down-regulating its catalytic activity. To explore this possibility, we compared chemical modification of SCCA2-treated or BSA-treated Der p 1 by biotin-conjugated maleimide, a cysteine residue-modifying reagent. Modification of SCCA2-treated Der p 1 by biotin-conjugated maleimide was reduced when compared with the level of BSA-treated Der p 1 (56 ± 14%, n = 3, Fig. 4*C*). These results suggest that down-regulation of the catalytic activity of Der p 1 may be due to its conformational change, although we cannot exclude the possibility that the cysteine residue of the active center was unexpectedly modified by SCCA2.

Resistance of SCCA2 against Cleavage by Der p 1—Although the irreversible conformational change of Der p 1 contributed to the inhibition mechanism of SCCA2, it could not fully explain it because fractionated Der p 1 still showed catalytic activity at the reducing level (Fig. 4*B*). As only intact serpin sustains its inhibitory activity in the suicide substrate-like mechanism, it would be possible that the difference of susceptibility to cleavage by the target proteinase could affect the inhibitory activity of serpin. To explore this possibility, we analyzed the digestion profile of SCCA2 in the presence of Der p 1 in a time-dependent manner. It turned out that SCCA2 was resistant to digestion by Der p 1 when compared with SCCA1 and that 53% of SCCA2 still existed, intact, after 30 min of incubation (Fig. 5). When SCCA1 was incubated with papain, intact SCCA1 immediately began to decrease and was completely lost within 15 min. These results demonstrated that resistance against the cleavage by the target proteinase was a unique property of SCCA2, and it could at least partially explain why SCCA2 exerted its potent inhibitory activity on Der p 1 when compared with SCCA1.

Preference of Amino Acids in the RSL Sequences of SCCA2 and SCCA1 for Inhibitory Effect on Der p 1—The distinct properties of SCCA1 and SCCA2 regarding the inhibitory effects on Der p 1 are assumed to be due to the difference of their RSL sequences. Actually, swapping the RSL of SCCA1 for that of SCCA2, or *vice versa*, revealed that the inhibitory effect on Der p 1 was dependent on the RSL of SCCA2 (Table II, SCCA1 RSL2, SCCA2 RSL1). We then exchanged each amino acid specific for the RSL of SCCA2 with that corresponding to SCCA1 and analyzed its inhibitory effect on Der p 1 (Table II). When Val-351, Val-352, or Leu-354 was replaced with Gly, Phe, or Ser, respectively, all of the mutated types attenuated the inhibitory effect (SCCA2 mut1, SCCA2 mut2, SCCA2 mut4), demonstrating that these residues were critical. Surprisingly, when Glu-353 or both Ser-356 and Pro-357 were exchanged with Gly or Pro and Thr, respectively, the inhibitory effect was augmented when compared with native SCCA2 (SCCA2 mut3, SCCA2 mut5). Furthermore, when Glu-353, Ser-356, and Pro-357 were all replaced with Gly, Pro, and Thr, respectively, the inhibitory action was dramatically up-regulated (Fig. 6, *A* and *B*, SCCA2 tm). Although Glu-353 was exchanged with Ala or Gln instead of Gly, the inhibitory effect was more enhanced than native SCCA2 (SCCA2 E353A, SCCA2 E353Q), indicating that removal of the ionic strength of Glu-353 would be important for up-regulation of the inhibitory effect. Furthermore, as switching of Pro-356 of SCCA tm with Ala did not influence the activity, Pro-356 in SCCA2 tm would not be critical, but removal of Pro-357 from native SCCA2 would be important (SCCA2 tm P356A). Finally, we confirmed that swapping of the RSL of SCCA tm for that of SCCA1 still sustained its potency,

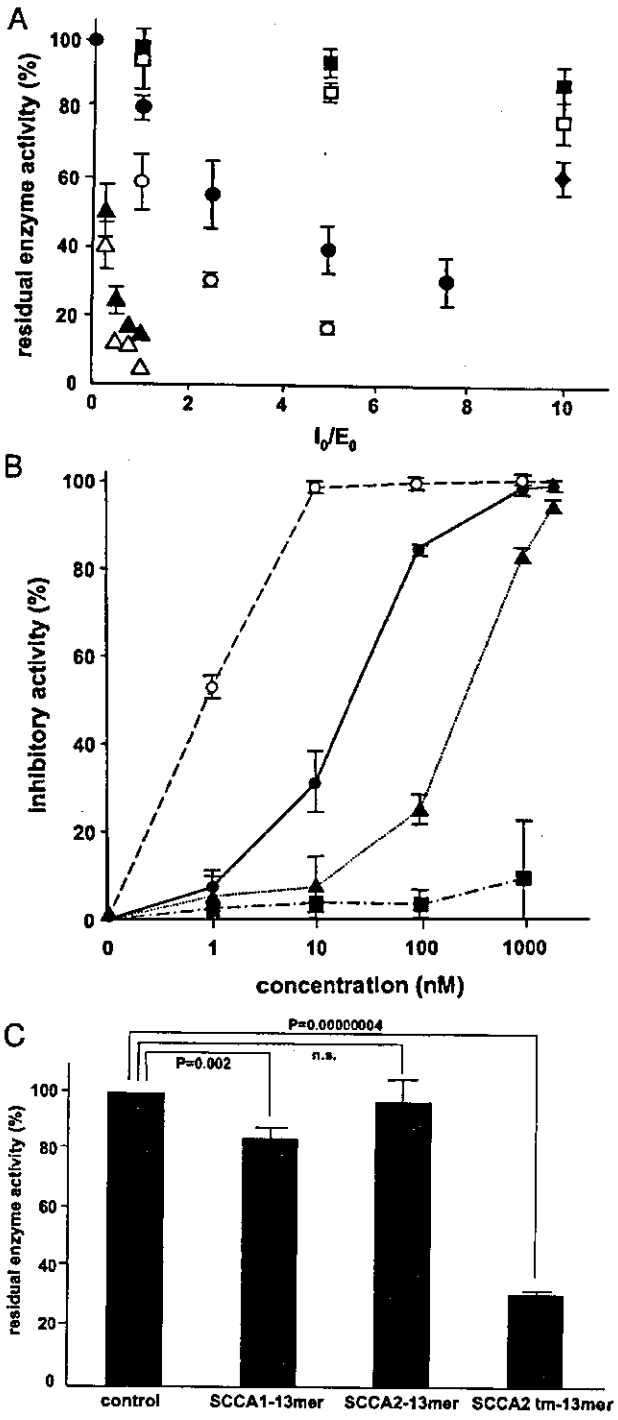

FIG. 6. **Inhibitory effects of SCCA2 tm on the catalytic activity of Der p 1.** In *A*, SCCA2 tm (*triangle*) was incubated with 10 nM Der p 1 (*closed*) or Der f 1 (*open*) at the indicated I_0/E_0 ratio, as shown in Fig. 1. In *B*, SCCA2 tm (*open circles*) was incubated with the indicated concentrations of Der p 1 at the I_0/E_0 ratio = 1, as shown in Fig. 1. The results of Fig. 1, *A* and *B*, are superimposed. In *C*, 10 nM Der p 1 was incubated with a 1:1000 ratio of each synthetic peptide for 30 min at 25 °C. Residual enzyme activities are depicted.

demonstrating the importance of the amino acid sequence of the RSL (SCCA1 RSL2 tm, data not shown).

To validate the importance of the amino acid sequence of the RSL in SCCA2 tm, we generated synthetic peptides corresponding to the RSLs of SCCA1, SCCA2, and SCCA2 tm, and then analyzed their inhibitory effects. At 1:1000 ratio, the peptide corresponding to SCCA2 tm, but not the peptides corresponding to SCCA1 and SCCA2, inhibited the catalytic activity of Der p 1 (Fig. 6*C*), again demonstrating the critical role of the sequence of the RSL in SCCA proteins.

Characterization of SCCA2 tm—We then compared the biochemical characteristics of SCCA2 and SCCA2 tm. It turned out that the biochemical properties of SCCA2 tm were almost the same as SCCA2. 1) It blocked the cleavage of CD25 by Der p 1 (data not shown). 2) It was cleaved by Der p 1 between Gly-353 and Leu-354 (data not shown). 3) It did not form a covalent complex with Der p 1 (data not shown). 4) SCCA2 tm caused irreversible inhibition on the catalytic activity of Der p 1 (33 ± 17%, n = 3, Fig. 4*B*), and incorporation of maleimide decreased to the same level as SCCA2 (48 ± 16%, n = 3, Fig. 4*C*). However, SCCA2 tm was more resistant to cleavage by Der p 1 than SCCA2 (67.5 ± 7.3% *versus* 53.1 ± 8.8% at 30 min, 68.0 ± 4.1% *versus* 47.7 ± 13.8% at 60 min, Fig. 5). These results demonstrated that the difference of resistance against cleavage by Der p 1 contributed to the different inhibitory activities of SCCA2 and SCCA2 tm.

DISCUSSION

In this study, we demonstrated that SCCA2 inhibited the cysteine proteinase activity of group I mite allergens, Der p 1 and Der f 1. Although it had been thought that SCCA2 targeted only serine proteinases, SCCA2 inhibits both serine and cysteine proteinases belonging to the cross-class serpin family, as well as CrmA, PI9, and SCCA1. It has been reported that Der p 1 performs various biological activities correlated with allergic reactions such as disruption of tight junction by cleaving occludin (25), secretion of inflammatory cytokines in bronchial epithelial cells by activating PAR-2 (26, 30, 31), and induction of Th2 subset by cleaving CD25 or CD40 (28, 29) *in vitro*. Although the precise pathological role of the catalytic activity of Der p 1 *in vivo* remains unclear, it is assumed that the cysteine proteinase activity of Der p 1 acts as a trigger or a worsening factor of bronchial asthma, based on the *in vitro* data. If this were the case, SCCA2 might play a protective role against group I mite allergens in the lesions of bronchial asthma, although IL-4 and IL-13, which induce expression of SCCA2 in bronchial epithelial cells, are themselves known to be involved in the pathogenesis of bronchial asthma (14, 15). The interaction between SCCA2 and group I mite allergens may help us elucidate the complexity of bronchial asthma. Alternatively, SCCA proteins might play a protective role against cysteine proteinases derived from parasites because it is known that some cysteine proteinases derived from *Leishmania mexicana* affect its virulence (37) and that IL-4/IL-13 protect against various parasites (38).

We next examined the inhibitory mechanism of SCCA2 on Der p 1, and the following events occurred. 1) SCCA2 was cleaved at the predicted site in its RSL (Fig. 3). 2) SCCA2 and Der p 1 did not form a complex with a covalent binding (Fig. 4*A*). 3) Interaction with SCCA2 partially impaired the catalytic activity of Der p 1, probably by irreversible conformational change (Fig. 4, *B* and *C*). The serpins employ a suicide substrate-like inhibitory mechanism in which the exposed RSL of the serpin is recognized by the proteinase, and then a "bait" peptide bond (P1-P1') that mimics the normal substrate of the proteinase is attacked by the active serine residue of the proteinase (12, 39). Upon the interaction, a standard serpin forms an acyl-enzyme intermediate with a serine proteinase linked by an oxy-ester bond. In its cleaved form, the P side of the RSL inserts into the body of the protein, which dramatically changes the conformations of the serpin and the proteinase, rendering it impossible for the ester bond to hydrolyze (36). We